

Decentralized Reliability Estimation for Mixnets

Claudia Diaz*

Harry Halpin[†]

Aggelos Kiayias[‡]

June 12, 2024

Abstract

Continuous-time decryption mixnets can anonymously route data packets with end to end latency that can be as low as a second, making them usable for a variety of applications. Such mixnets however lack verifiable reliability properties that ensure the correct processing and delivery of packets, while existing verifiability mechanisms are incompatible with scalable low latency continuous-time mixnets due to imposing overheads measuring in minutes to hours. This work addresses this gap by proposing a scheme that can estimate reliability scores for links and nodes forming a continuous-time mixnet where some form of credentials authorize clients to send traffic. The scores can be computed publicly by all participants from a set of measurement packets that are eventually revealed and act as a random sample of the traffic, without affecting mixnet transmission latency for client packets. Our scheme relies on VRF-based routing, a novel primitive that ensures that legitimate client packets follow the routing policy of the mixnet, as well as randomly generating unforgeable measurement packets. We experimentally validate our construction both in unreliable and adversarial settings, demonstrating its feasibility.

1 Introduction

Mix networks or *mixnets*, first introduced by Chaum [4], are a basic technique for anonymously routing packets through multiple intermediaries called *mix nodes*, such that the input and output packets of nodes are unlinkable due to cryptographic transformations and packet reordering. Mixnets route each packet independently, in contrast to Onion Routing [16] networks such as Tor [12] that establish end-to-end bidirectional circuits carrying all the packets of a communication flow — and providing the initiator with a live connection to each routing intermediary. Continuous-time mixnets [29] function by default as a *fire-and-forget* protocol, where packet delivery is not guaranteed and the sender lacks straightforward mechanisms to check the mix nodes acting as routing intermediaries for their packets. Reliable packet transmissions can be achieved with end-to-end acknowledgments and retransmissions [9]. Such solution however does not reveal which mix node in the path failed to process and forward a packet, neither provides a mechanism to publicly estimate the reliability of individual mix

nodes across all the clients’ traffic — information that is critical for network management that accounts for quality of service.

Mixnets *can* be designed to provide very high assurances with respect to correct processing by all mix nodes and final message delivery by having: (i) round-based communication, with clients normally sending at most one short message per round; (ii) all communications along the route happen via broadcast (or “bulletin board”), thus being publicly verifiable; and (iii) some form of verifiable shuffle at each mix node that allows it to publicly prove (via broadcast) the correctness of the mixing operation, before the next step of routing can proceed. These requirements, and the resulting latency, severely restrict the uses cases where these mixnets can be practically deployed. Voting applications are a common use case for these solutions [15, 27], given their strict integrity and verifiability requirements and their latency tolerance. More scalable and efficient mixnet designs within this paradigm have been proposed for implementing anonymous micro-blogging applications [22] or private client messaging via dead-drops [32, 23]. Even these faster designs however have a routing latency of minutes, which grows with the number of messages routed in the round, making them unsuitable to support diverse applications.

In this paper we consider scalable continuous-time mixnets such as Loopix [29] and Nym [9] that can deliver packets with a latency as low as a *sub-second*, so that the mixnet is practically usable for a broad range of applications including email, instant messaging, file sharing, broadcast of (blockchain) transactions, and general purpose internet access. Furthermore, packet’s end-to-end routing latency should not be affected as the network scales to handle more clients and packets. This can be achieved by mixnet architectures such as Loopix [29] where mix nodes process packets individually, rather than in round-based batches, and where clients can select the per-node delay of their packets from a latency distribution that is compatible with the latency tolerance of their application [18]. The Nym mixnet,¹ which is an implementation of Loopix with various extensions, currently delays packets by an average of 50ms at each of three hops, resulting in 500ms to 800ms end-to-end latency when network propagation delays are included. Packet processing times take less than 1ms and their contribution to total latency is negligible in comparison to mixing and propagation time.

Nym [9] includes several additional components compared to Loopix: (1) it implements anonymous credentials to authorize usage of the mixnet in terms of an allowance of

*KU Leuven and Nym Technologies SA, Belgium, cdiaz@esat.kuleuven.be

[†]Nym Technologies SA, Switzerland, harry@nymtech.net

[‡]University of Edinburgh and IOG, UK, aggelos.kiayias@ed.ac.uk

¹<https://explorer.nymtech.net>

packets given to subscribed clients [30]; (2) it includes both a blockchain for long-term data storage and an ephemeral broadcast layer that function as public bulletin board to register nodes, keep track of node staking and rewarding, coordinate network operations and provide a consistent view on the state of the network to all participants; (3) lastly, Nym relies on an incentive mechanism that rewards nodes taking into account their reliability, such that they miss out on rewards if they go offline or otherwise fail to process and forward packets [10]. This is reinforced by a reputation mechanism based on staking that further incentivizes stakeholders to delegate their stake to reliable nodes, which in turn increases their chances of participation in the network. Nodes found to be unreliable both lose immediate rewards and reduce their possibilities to participate in the network in the next epochs. Consistently underperforming nodes eventually lose stake from delegates that switch to more reliable (and profitable) nodes, diminishing the reputation, future rewards, and chances of participation of the underperformers. Note that newly created nodes may need time to build reputation, and thus nodes are incentivized to maintain long-term identities.

Running the Nym incentive mechanism therefore requires computing a ‘reliability’ or ‘performance’ score per node participating in the mixnet. This must be done in a context where packet transmissions between a pair of parties are one-to-one (instead of via shared broadcast) and thus, if the sender and receiver of a transmission disagree, no third parties can verify whether a packet was never sent, sent but not received, or sent and received but not acknowledged as received. Furthermore, in this setup mix nodes are not able to publicly prove that their outputs are legitimate transformations (shuffles) of their inputs. Thus, if packets are dropped or substituted along routes it is generally not trivial to determine who is deviating from the protocol. Due to the lack of existing decentralized solutions, which has long been an open problem in mixnet research [13], current performance estimations in the Nym mixnet rely on a trusted measurement authority that sends test packets to itself to compute performance estimates, which makes all estimates and resulting rewards vulnerable to a faulty or malicious authority.

This work addresses this open problem by proposing a scheme that can estimate the reliability of all the mixnet links and nodes in a decentralized manner — at a fraction of the per-packet overhead and latency offered by verifiable shuffling techniques, while still relying on broadcast to achieve public verifiability. Assuming that clients obtain (anonymous) credentials [30] that entitle them to send an amount of legitimate traffic through the mixnet, our solution further ensures that clients follow the mixnet’s stated routing policy when privately creating legitimate packets. We design our scheme to be compatible with the Nym network, while keeping it as generic as possible so it can be analyzed in a stand alone manner.

Our design is built using a novel primitive that we call *VRF-based routing*. A VRF (Verifiable Random Function) [26] is a function that maps any input to a pseudo-random value in a way that is publicly verifiable. Based on VRFs we show how we can tie each legitimate packet to a valid client credential and ensure that its route is ran-

domly chosen according to the mixnet’s publicly known routing policy. VRF-based routing further allows turning a mixnet’s packet encoding scheme (such as the widely deployed Sphinx [7] format used by Loopix and Nym) into a verifiably unbiased lottery for *measurement packets* that are used for network monitoring purposes rather than for carrying client data. The intuition is that of an undercover “secret shopper” that goes to a store to detect malicious or faulty behavior in employees, a concept that has been proposed earlier to probabilistically catch misbehaviour in a mix cascade setting [13]. Measurement packets are indistinguishable from normal packets while in transit, but they can be revealed and verified at a later stage to facilitate legitimate traffic estimates. Taking advantage of this, we introduce a protocol that periodically produces public estimates for the share of legitimate traffic transmitted and dropped at each mixnet link during a time epoch. We further propose a method to estimate node performance scores from link performance.

We empirically evaluate via simulations the proposed protocols. We show that, in the presence of random node failures and given sufficient measurement samples, our node performance estimation protocol produces accurate estimates. Furthermore we show that malicious nodes that attempt to lower their neighbours’ estimates by selectively dropping packets pay a performance cost equivalent to the cost inflicted on their targets, thus neutralizing “creeping death” attacks [13] where adversaries gain relative reputational advantage over time. The proposed protocols are highly scalable with increases in the client base, as the amount of measurements and related overheads remain constant for a desired estimation accuracy and network size, rather than growing proportionally to the amount of client traffic or the size of packets.

Paper organization. We first introduce the problem statement in Sect. 2 by describing the system and threat models and the desired properties. In Sect. 3 we describe the core elements of our scheme, including a protocol that estimates mixnet link performance and the *VRF-based routing* primitive that is a key building block of our solution. We show in Sect. 4 how link performance estimates can be further processed to compute performance estimates for mix nodes, where we evaluate the accuracy of the proposed methods via simulations, as well as the overhead of a possible implementation. Finally, we review related work in Sect. 5 and conclude with future avenues of research in Sect. 6.

2 Model and Problem Statement

2.1 System Model

Decryption mixnet model. We consider a *decryption mixnet* where senders prepare packets by encrypting them with the keys of selected intermediaries, each of which then removes a layer of encryption when routing the packet. We abstract the mixnet topology as a labelled directed graph G . Vertices are labelled as either *mix nodes*, *gateways* or *clients*. Edges in G represent the communication links between these entities. We denote the edge from vertex i to j as $e = (i, j)$. Mix nodes have both incoming and

outgoing edges to other mix nodes and gateways. Gateways serve both as entry and exit points with respect to the mixnet and have incoming and outgoing edges to both mix nodes and clients. For each entity j we define as $P(j)$ the set of its immediate predecessors and $S(j)$ the set of its immediate successors in G . The set of “forward direction predecessors” denoted by $P^*(j)$ is defined to be \emptyset for a client j , a set of clients in case j is a gateway, and $P^*(j) = P(j) \cup_{i \in P^*(j)} P^*(i)$ for a mix node j . A packet route is initiated by a client that is affiliated with a gateway g_0 and follows a path in G picking outgoing edges and traversing multiple mix nodes. The last mix node in the path is followed by the recipient’s gateway g_1 , who delivers the packet to its intended destination, which could be another client, a service, or a proxy to the open internet.

Client credentials. Users buy a *subscription* by performing a payment on a smart contract on the blockchain. This subscription has the form of a compact e-cash wallet [31] (with keys $vk_{\text{long}}, sk_{\text{long}}$) that contains a bundle of N unlinkable *credentials*. Each credential c entitles the client to route up to S_c packets through the mixnet.

Network and routing policy. We assume for convenience that the mixnet graph G has a layered topology, i.e., $N = LW$ mix nodes are arranged in L layers, with each layer having W nodes. Mix nodes are selected² from a pool of at least N eligible nodes and assigned randomly to a layer for a time period (*epoch*), with the node selection being refreshed every new epoch so that nodes rotate positions and underperforming nodes can be replaced. The set of W_G gateways that act as interface between clients and the mixnet is assumed to remain relatively stable over time to minimize the need for clients to switch gateways with the change of epoch, though gateways may be replaced, e.g., if they have low popularity among clients or low performance. Nodes in the first layer of the mixnet only accept packets from eligible gateways and clients only spend credentials with eligible gateways of their choice.

The routing policy is such that valid routes include one node per mixnet layer independently selected with probability $\frac{1}{W}$. The layers are ordered and valid packet routes traverse them in the same order: nodes in the first layer receive input packets from gateways and forward them to nodes in the second layer, who in turn forward them to the third layer. This is iterated until packets reach the nodes in the last (L -th) layer of the mixnet, at which point they are forwarded to their corresponding destination gateway.

Blockchain and broadcast channel. We assume that all nodes have access to a blockchain setup that enables them to post transactions that are stored and available long term. Additionally, nodes can use a “layer 2” ephemeral broadcast channel that enables one-to-many information dissemination for information that only needs to be available for a limited time. Using this layer will be referred to as “broadcasting.” This component is instantiated in the Nym mixnet by the use of a Cosmos-based blockchain with the ‘Ephemera’ layer 2 solution that serves as a general purpose key-value pair database on the blockchain whose state can be reset

²If more than N nodes are available, the selection criteria accounts for node reliability and reputation, as is the case in Nym, so that underperforming nodes are excluded.

every few epochs. The code is available online.³

2.2 Threat Model

We consider a threat model that features the following.

- The adversary may control multiple clients and a limited number of mix nodes and gateways. Malicious mix nodes can adaptively drop or substitute packets as well as lie when broadcasting output values. Active malicious behaviour by gateways is assumed to be utility maximizing: gateways follow any strategy as long as it does not decrease their utility. We allow any utility function to be used for gateways as long as it is monotonically increasing on a number of indicators — defined precisely in Section 3.2.
- “Honest” nodes (mix nodes and gateways) are divided in a set of reliable nodes that are consistently online and process all received packets and a set of unreliable nodes which experience downtime, throughput limitations, or other faults that result in packet drops. All honest nodes report true output values in every epoch.
- A credential issuer that issues credentials as requested but is not trusted with respect to the privacy of clients.
- A blockchain and ephemeral broadcast channel that cannot be subverted by the adversary, i.e., they satisfy consistency: honest parties have the same view regarding their contents (perhaps subject to a lag between them due to catching up with protocol messages at different times), as well as liveness, i.e., given sufficient time after a transaction is posted either on the ledger or the ephemeral broadcast channel, the transaction is available for all to have access to. Note that in the case of the ephemeral broadcast channel, unreliable honest parties may miss transmitted messages, while in the case of blockchain all honest parties eventually catch up on all posted transactions.

2.3 Properties

There are two cryptographic algorithms that typify every mixnet: the *packet encoding* algorithm that prepares content to be routed via the mixnet and a *packet processing* algorithm that is executed at every hop in the packet route. In a paid service setting, these two algorithms are further equipped with the characteristic that there is a limited amount of bandwidth that a user is authorized to use. Prior to running the packet encoding algorithm, clients obtain their e-cash wallet which provides them with an (anonymous divisible) bundle of N credentials; subsequently, they approach a gateway and, using the divisibility property of their subscription, spend one of the N credentials that will entitle them to submit S_c packets to that gateway, who in turn forwards them to the mix nodes. Packets that originate from a particular credential and gateway and are encoded correctly using the packet encoding algorithm are called

³<https://github.com/nymtech/nym/tree/develop/ephemera>

legitimate packets. Note that a legitimate packet is well-defined given the gateway identity, the credential keys and the random coins used by client and gateway assuming both are running the mixnet encoding algorithm.

Given this feature, for each epoch, we associate the following quantities with a link e : s_e is the number of legitimate packets that were successfully transmitted, i.e., sent and received across the link e , and d_e is the number of legitimate packets dropped in the link. We consider that $d_{(c,g)} = 0$ in the link $e = (c, g)$ between client and gateway, and that $s_{(c,g)}$ thus includes all the packets generated from the client’s credential c . At each next step of the path, the quantities s_e and d_e of the incoming and outgoing links of a gateway or node j satisfy the following relation.

$$\sum_{i \in P(j)} s_{(i,j)} = \sum_{k \in S(j)} s_{(j,k)} + d_{(j,k)} \quad (1)$$

where $\sum_i s_{(i,j)}$ represents the number of packets received by j from all its predecessors, $\sum_k s_{(j,k)}$ are the packets successfully transmitted to all its successors, and $\sum_k d_{(j,k)}$ are the packets received by j but dropped before reaching their next destination.

Definition 1. A mixnet with reliability estimation (REst-mixnet) is a mixnet scheme over a graph G where (1) time is divided in epochs; (2) in each epoch a publicly known number of legitimate packets are introduced through each gateway; and (3) given an edge $e = (i, j)$, all participants are able to estimate the link’s performance ρ_e , defined as the fraction of legitimate packets successfully transmitted from i to j , relative to all the legitimate packets received by i to be forwarded to j ; i.e., including both the s_e packets that were successfully received by j and the d_e packets that were dropped before being registered by j :

$$\rho_e = \frac{s_e}{s_e + d_e} \quad (2)$$

An estimation $\hat{\rho}_e \approx \rho_e$ can be obtained by anyone who reads the broadcast channel. For a given confidence level (Z-score), the accuracy of the estimation is bounded by a per-link maximum error ϵ_e which is computed in tandem with $\hat{\rho}_e$.

In other words in a REst mixnet, parties are able to estimate the rate of successfully transmitted legitimate packets in individual links and even along multi-link paths of interest in the mixnet graph. At the same time, we require the following two security properties.

Replay Protection. This property ensures that legitimate packets can only be processed *once* by mixnodes. This is a common property in decryption mixnets [6, 29] where each packet leaves a fingerprint that can be recognized in case of replay, so that duplicates can be identified and dropped by the receiving node.

Privacy. Finally, the main objective of any mixnet is to provide unlinkability between input and output packets, assuming an adversary that knows the sender and receiver sets, observes traffic in all the network links (including between clients and gateways) and even controls some of the participants. The reliability estimation mechanism should not leak any *additional* information to the adversary that could be useful to deanonymize packets.

3 Performance Estimation Protocol

We design a REst mixnet by introducing indistinguishable measurement packets into the traffic of the mixnet that are subsequently opened and traced along the paths in the mixnet graph. We lay out the description of our protocol in two parts. First, we describe a sampling protocol that generates measurement traffic and enables mix nodes to present evidence regarding their performance; this allows the performance estimation algorithm that pulls together the broadcast information to estimate the ratio of successfully transmitted packets in each link and its associated error given a confidence interval; this approach works in a setting where clients and gateways are semi-honest. Second, we introduce VRF-based routing, which is a cryptographic tool that generates unforgeable measurement packets according to the routing policy and limits attacks by malicious clients and gateways.

3.1 Link performance estimation

We start by describing our link estimation protocol in the simpler setting where clients and gateways are (semi) honest. Then, we show how VRF-based routing can mitigate deviations by clients and gateways.

Generation of packets. A client spends (from the subscription bundle of N unlinkable credentials) a credential c with a gateway g , entitling the client to route S_c packets through the mixnet via g . For each packet transmission, a coin is flipped between the client and the gateway and with probability p_{lot} the packet transmission opportunity is used to send a measurement packet. As routing intermediaries, mixnet nodes cannot distinguish measurements from regular packets, which are only distinguishable by the packet recipient.

Let $s_{(c,g)} \leq S_c$ denote the total number of packets generated from c that have been routed by g within the epoch (note that $s_{(c,g)} = S_c$ when the credentials’ entire allowance is consumed within one epoch, which will often be the case if S_c is small, and also that each c is unlinkable to any other credential from the same subscription). The number of generated measurement packets $s_{(c,g)}^*$ follows a binomial distribution $s_{(c,g)}^* \sim B(s_{(c,g)}, p_{\text{lot}})$, and thus we can expect $s_{(c,g)}^* \approx p_{\text{lot}} \cdot s_{(c,g)}$. Measurement packets are sent as they appear, interleaved with the rest of the client traffic, while measurement packet openings are kept by g (and potentially also by c) for later disclosure.

Routing of packets. Gateways send packets to the first-layer mix node specified as first hop of in each packet’s route. Mix nodes execute the *packet processing* algorithm and further relay packets to their next destination. As part of replay protection in mixnets, mix nodes must record a *tag* per processed packet (denoted by t , cf. Sect. 3.2). A newly received packet is then checked against the list of tags already seen: if the packet is fresh, it is processed and its tag is added to the list; and otherwise the packet is dropped. Each node j uses a Bloom filter [2] to store in a space-efficient manner the $\sum_i s_{(i,j)}$ tags received from its predecessors $i \in P(j)$ during an epoch. When adding a fresh packet tag to the Bloom filter nodes first append a binary flag, indicating whether the packet integrity checks where correct,

allowing the packet to be further relayed; or incorrect, forcing node j to drop the packet. Mix node decryption keys are updated per epoch to provide forward security in addition to ensuring that packets cannot be replayed in a later epoch.

Measurement packets have as destination a randomly selected gateway with the probability weights being part of the mixnet’s routing policy. When gateways receive a measurement packet, they store its tag in a locally maintained Bloom filter and proceed to discard the packet. Note that gateways do not need to store in the Bloom filter the tags of non-measurement packets, meaning that their Bloom filters can be smaller than those of mix nodes.

Post-epoch stage: revelation of measurements. Once an epoch has ended, the protocol proceeds in three steps:

1. Each gateway g broadcasts the number of packets $N_{g,c}$ sent per credential c .
2. All nodes and gateways broadcast their Bloom filters.
3. Gateways reveal the openings of the $s_{(c,g)}^*$ ($\approx p_{\text{lot}} \cdot s_{(c,g)}$) measurement packets sent from each credential c they have serviced in the epoch.
4. Any entity reading broadcast outputs can verify the validity of the gateway openings and use them to recreate the $\sum_g \sum_c s_{(c,g)}^*$ measurement packets generated in the epoch. As result, the path and recipient of each measurement packet, as well as the tags seen at each step of the route, become available. All entities can then check which measurement packet tags were included in the Bloom filters broadcast by mix nodes and gateways in step (1).

Given a link (i, j) in the mixnet, we denote by $s_{(i,j)}^*$ the amount of measurement packets *successfully transmitted* in the link, and compute it by counting the measurement packets whose (per-hop) tags appear in the Bloom filters of both i and j . On the other hand, the quantity $d_{(i,j)}^*$ denotes the number of measurement packets *dropped* in the link, computed by counting the measurement packets whose tags appear in the Bloom filter of i but not in the one of j . For every intermediary node j it holds that packets received from all predecessors i are either successfully transmitted to their next destination k , or dropped before reaching k :

$$\sum_i s_{(i,j)}^* = \sum_k s_{(j,k)}^* + d_{(j,k)}^* \quad (3)$$

In the case of gateways, measurement packets revealed by g that do not appear in the Bloom filter of the corresponding first layer node i are considered as part of $d_{(g,i)}^*$. Similarly, measurement packets addressed to g from last layer node k that are reported by k but do not appear in g ’s Bloom filter, are considered part of $d_{(k,g)}^*$.

Packets reported as dropped due to failed integrity checks (as indicated by the flag stored with the tag) are entirely removed from the measurement sample set. Similarly, packets with ‘holes’ in their reported paths, i.e., included in node j ’s Bloom filter but missing from its predecessor, are also entirely discarded as measurements.

Taking into account that mixnet intermediaries cannot distinguish measurement from regular packets while routing, measurement packets are transmitted and dropped by

nodes at the same rate as any other packet. We use this to produce an *estimated performance* $\hat{\rho}_e$ for link e , given by the transmitted and dropped samples s_e^* and d_e^* :

$$\hat{\rho}_e = \frac{s_e^*}{s_e^* + d_e^*} \quad (4)$$

The accuracy of $\hat{\rho}_e$ as an estimator of ρ_e depends on the available number of measurement samples $s_e^* + d_e^*$, which determine the maximum sampling error ϵ_e with a given a confidence level, such that:

$$|\rho_e - \hat{\rho}_e| \leq \epsilon_e \quad (5)$$

To bound the estimation error ϵ_e we use methods that estimate coin bias from a sequence of observed coin flips, considering that the coin flip can result in transmission (heads) with probability ρ_e ; or in a drop (tails) with probability $1 - \rho_e$. Given an edge with $s_e^* + d_e^*$ observed coin flips and confidence level Z , the maximum estimation error ϵ_e is given by:

$$\epsilon_e = Z \cdot \sqrt{\frac{\rho_e \cdot (1 - \rho_e)}{s_e^* + d_e^*}} \approx Z \cdot \sqrt{\frac{\hat{\rho}_e \cdot (1 - \hat{\rho}_e)}{s_e^* + d_e^*}} \quad (6)$$

The maximum estimation error occurs when $\rho_e = 0.5$, and thus $\epsilon_e \leq \frac{Z}{2\sqrt{s_e^* + d_e^*}}$ for any value of ρ_e , with the error diminishing significantly when ρ_e approaches zero or one. Since ρ_e is not available, in practice we use $\hat{\rho}_e$ when computing ϵ_e as best available approximation of ρ_e . In cases where $\hat{\rho}_e = 1$ or $\hat{\rho}_e = 0$, we use Laplace’s *rule of succession* to estimate $\epsilon_e \approx \frac{1}{s_e^* + d_e^* + 2}$.

Note that the estimation accuracy for edge e is dependent on the number of measurement samples $s_e^* + d_e^*$ but **not** on the total number of packets $s_e + d_e$. The method thus requires an amount of measurement samples per link to have a certain accuracy, which stays **constant** regardless of the amount of total traffic. Thus, as more traffic is routed in the network, the percentage p_{lot} of measurement packets can be decreased while maintaining accuracy. The output of this protocol is a value $\hat{\rho}_e \approx \rho_e$ per edge that estimates the link performance, defined as the fraction of successfully transmitted packets, together with a corresponding sampling error ϵ_e that qualifies the accuracy of the estimation for a given confidence level.

Privacy. Aside from the total number of packets sent in an epoch on behalf of each credential, which is already available to a network adversary, the scheme does not reveal any other information about the clients. Note that credentials are not linkable to each other, nor to long-term client subscriptions or identities, and thus cannot be exploited for long-term profiling of client activity volume. Note also the tradeoff between credential size (in terms of number of packets S_c) and privacy: a smaller S_c better disaggregates usage by a single client, while incurring more overhead in terms of credential verification (as more small credentials need to be verified when sending a large number of packets). Ideally, credentials have a size S_c that is easily consumed within a single epoch.

k : security parameter; length of the hash function output.
p_{lot} : probability of a measurement packet.
ctr : packet counter
r_{type} : randomness for measurement lottery.
r_{pkt} : randomness for packet encoding.
y_n : public-key of node n
T : target that determines measurement lottery outcome
s_i : Diffie Hellman key corresponding to packet hop i
b_i : blinding value corresponding to packet hop i
\tilde{r}_i : encoding randomness for packet hop i
n_i : node corresponding to packet hop i
n : unpredictable random nonce drawn from public source
α_i : base element for packet hop i
ψ_i : ciphertext for packet hop i
x_i : secret-key of processing node in packet hop i
t_i : pseudorandom tag calculated in packet hop i

Table 1: Notations for VRF-based routing.

3.2 VRF-Based Routing

In this section we show how to transition our protocol to the full threat model that considers gateways to be utility maximizers while clients may be malicious. Specifically, we consider gateway utility to be a monotonically increasing function⁴ of (i) link performance, as measured by the protocol itself, for all the mixnet links that gateways are a counterparty to, (ii) client satisfaction, a ratio between the packets that an honest client successfully sends and are delivered divided by the total number of packets the client requests to be sent, (iii) credential consumption, the total number of announced legitimate packets sent, and (iv) not getting caught cheating in any of the requested public operations. The gateway being a utility maximizer means that it in all cases will avoid strategies that reduce its utility but may choose any strategy that maximizes its utility.

Viewed in this setting, the scheme of the previous section can be easily seen to be ineffective. For instance, given that measurement packets are not subject to integrity checks, it is possible for a gateway to follow the protocol as described, but then open as measurement packets some other packets that only partially match the sent measurements. In that case, the performance in the links where the gateway is a counterparty will be correct but performance estimations for other links will be lower, given that incorrect tags are revealed for some hops and thus it seems that the measurements got dropped further in their path. At the same time, since clients can be malicious we cannot rely on them entirely for generating the measurement traffic. To mitigate these issues, we introduce VRF-based routing, where the measurement packets are provably stochastically generated across an epoch’s packet transmissions, emulating indepen-

⁴Nym’s reward function [10] can easily be configured for gateways to increase monotonically with all these variables.

dent coin flips.

VRF-based routing. VRF-based routing relies on two primitives. First, a VRF function that consists of three algorithms $\langle K, E, V \rangle$: K generates a key pair (sk, vk) ; $E(sk, m) = (r, \pi)$ evaluates the VRF on m to produce the pseudorandom output $r \in \{0, 1\}^k$ as well as a proof π ; and $V(vk, m, r, \pi)$ verifies that r is the correct output corresponding to the message m . Second, a mixnet encoding scheme that sets the individual hops in a packet’s path. For brevity we do not provide a formal syntax for the mixnet encoding; for an example, see Sphinx [7]. Our construction also takes advantage of non-interactive zero-knowledge proofs, for which we use standard notation, e.g., $\text{NIZK}(g, y \exists x : g^x = y)$.

We describe VRF routing with respect to a public algorithm $\text{Routing}(n, r)$ that for a given mixnet node n and randomness r samples the node that should be the next recipient after n , assuming r is uniformly distributed over $\{0, 1\}^k$. A common choice for Routing is to sample uniformly at random from a set of nodes identified as the *successor* nodes of n in the mixnet graph G .

We illustrate the concept of VRF routing in two steps. First, we describe how encoding works w.r.t. a public unpredictable nonce n , an integer target value $T = p_{\text{lot}} \cdot 2^k$, where $p_{\text{lot}} \in (0, 1)$, a packet counter ctr of maximum ℓ_{ctr} bits, and a Hash function $H(\cdot)$ modeled as a random oracle. Suppose the sender has selected an entry gateway n_0 with key y_0 and an exit gateway n_ν , where $\nu > 0$ is the number of packet hops. The gateway has already established a VRF key (vk, sk) , and the client a (packet) randomization key $(\alpha = g^x, x)$. The gateway computes three VRF values $r_{\text{pkt}} = E(sk, n || ctr || \text{pkt})$, $r_{\text{exit}} = E(sk, n || ctr || \text{exit})$, $r_{\text{type}} = E(sk, n || ctr || \text{type})$, where pkt , type , exit are the numerical labels $\{0, 1, 2\}$; note we use $||$ to denote concatenation. In case $r_{\text{type}} < T$, then the packet associated with ctr is a *measurement packet*, otherwise we have a *regular packet*. In the latter case, the sender receives the VRF values from the gateway, and calculates $\alpha_0 = \alpha^{r_{\text{pkt}}}$, $s_0 = y_0^{r_{\text{pkt}} \cdot x}$, $\tilde{r}_0 = H(\text{rnd}, s_0)$, $r_0 = H(\text{next}, s_0)$, $b_0 = H(\text{bli}, s_0)$, where rnd , next , bli are the numerical labels $\{3, 4, 5\}$ respectively. Subsequently (for $i = 1, \dots, \nu$), $\alpha_i = \alpha_{i-1}^{b_{i-1}}$, $s_i = y_i^{r_{\text{pkt}} \cdot x}$, where y_i is the key of node $n_i = \text{Routing}(n_{i-1}, r_{i-1})$ (for $i < \nu$), and finally, as before, $\tilde{r}_i = H(\text{rnd}, s_i)$, $r_i = H(\text{next}, s_i)$, $b_i = H(\text{bli}, s_i)$. In the above, we have the exception that y_ν is the key of the exit gateway (and hence n_ν is not selected as $\text{Routing}(n_{\nu-1}, r_{\nu-1})$). In the case of the measurement packet, the procedure is the same with the distinction that $x = 1$ in the calculations provided above, i.e., the randomness key α is not involved and as a result $\alpha_0 = g^{r_{\text{pkt}}}$ and the gateway can calculate the measurement packet independently. Moreover, the exit gateway is redefined randomly by $n_\nu = \text{Routing}(n_{\nu-1}, r_{\nu-1} \oplus r_{\text{exit}})$, where \oplus stands for exclusive-or. In either case, the above process enables to apply the mixnet encoding along the route $\langle n_0, \dots, n_{\nu-1}, n_\nu \rangle$, using randomness \tilde{r}_i at the i -th hop. The resulting packet is augmented with the value α_0 . The packet construction is illustrated in Figure 1. Note that the packet counter ctr is incremented with each packet.

Second, the processing of a packet (α_0, ψ_0) corresponding to VRF values $r_{\text{pkt}}, r_{\text{type}}$ proceeds as follows. The gate-

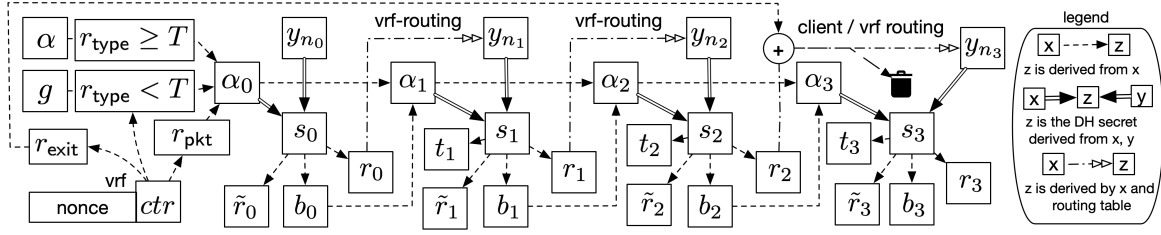


Figure 1: Illustrating the dependencies between the packet variables $\alpha, b, s, r, t, \tilde{r}$ when processing a VRF-based routing packet in the case of $\nu = 2$. The measurement packet condition is illustrated in the upper left.

way calculates $s_0 = \alpha_0^{x_0}, \tilde{r}_0 = H(\text{rnd}, s_0)$, where x_0 is its secret-key and it verifies that: (I) the mixnet encoding was correctly applied to produce ψ_0 given randomness \tilde{r}_0 and the public key y_0 ; and (II) the per packet randomization key is correctly computed: in the case of a non measurement packet it is $\alpha_0 = \alpha^{r_{\text{pkt}}}$, while it is $\alpha_0 = g^{r_{\text{pkt}}}$ in the case of a measurement packet. If these checks pass, it calculates the next hop as $n_1 = \text{Routing}(n_0, r_0)$, where $r_0 = H(\text{next}, s_0)$ and then it forwards (α_1, ψ_1) to node n_1 , where $\alpha_1 = \alpha_0^{b_0}$ with $b_0 = H(\text{bli}, s_0)$ and ψ_1 is the payload of packet ψ_0 after processing it in the way the mixnet decoding requires.

Next we illustrate how processing works for the remaining nodes in the path. Node n_i , given (α_i, ψ_i) for $i = 1, \dots, \nu$ operates as follows. First, it processes the packet to reveal payload ψ_{i+1} and if $i < \nu$, the next hop n_{i+1} . Then it calculates $s_i = \alpha_i^{x_i}, \tilde{r}_i = H(\text{rnd}, s_i)$, and if $i < \nu$, $\alpha_{i+1} = \alpha_i^{b_i}$ where $b_i = H(\text{bli}, s_i)$. The node then verifies that (I) the mixnet encoding was correctly applied to produce ψ_i given randomness ρ_i , (II) in case $i < \nu - 1$ $n_{i+1} = \text{Routing}(n_i, r_i)$ where $r_i = H(\text{next}, s_i)$, (the randomized routing check). It also calculates the tag $t_i = H(\text{tag}, s_i)$, and stores (b_i, flag_i) in a database of processed tags where flag_i is 1 if and only if the integrity check of ψ_i is valid. Finally, if $i < \nu$, it forwards $(\alpha_{i+1}, \psi_{i+1})$ to node n_{i+1} . Finally, in case $i = \nu$, the payload $\psi_{\nu+1}$ is parsed as the plaintext and is processed by node n_ν .

The key point of the above construction is that the randomness used for encoding is pseudorandomly determined by the key α and the VRF function. Specifically, for each ctr , there is a per packet randomization key $\alpha_0 = g^{x \cdot x_0 \cdot r_{\text{pkt}}}$ that is used to seed the mixnet encoding. For measurement packets, observe that the gateway can completely validate their computation due to the fact that r_{pkt} is known and the secret randomization key x of the client is not used in the packet calculations. The same holds true for any party that obtains the value r_{pkt} . Furthermore, any packet can be demonstrated to be a measurement or not, by checking the inequality $r_{\text{type}} < T$ which is true iff the ctr value corresponds to a measurement packet.

The following theorem is a straightforward observation regarding the construction. The first and third statement follow easily from the Diffie Hellman assumption, while the second takes advantage of the random oracle and the fact that routing choices depend on the unpredictable value nonce. Due to lack of space a proof is sketched in the appendix.

Theorem 1. *Assuming the pseudorandomness of the VRF,*

the Decisional Diffie Hellman assumption and that $H(\cdot)$ is modeled as a random oracle, (I) the VRF-based encoding presented above does not interfere with the security or the privacy of the underlying mixnet encoding scheme. (II) the packet routes generated by the above process are sampled according to $\text{Routing}()$ pseudorandomly, even in the setting where vk, α are adversarially chosen. (III) assuming client and gateway are honest, the measurement packets are computationally indistinguishable to non-measurement packets.

Deploying VRF-based routing. The concept of VRF-based routing is deployed utilizing (I) a threshold compact e-cash scheme [31], (II) a VRF function based on Dodis Yampolskiy’s PRF [14]; specifically, K produces a secret key sk_{vrf} and public-key $vk_{\text{vrf}} = g^{sk_{\text{vrf}}}$, while the VRF evaluation is set to $E(n||ctr||\text{label}) = (r_{\text{label}}, \pi)$ where $r_{\text{label}} = H(vk_{\text{vrf}}, g, u_{\text{label}})$, $u_{\text{label}} = g^{1/(sk_{\text{vrf}} + 2^\ell n + 2 \cdot ctr + \text{label})}$, and $\pi_{\text{label}} = (u_{\text{label}}, \pi'_{\text{label}})$ where and $\pi'_{\text{label}} = \text{NIZK}(g, vk_{\text{vrf}}, u_{\text{label}}, ctr, \ell, \text{nonce}, \text{label} : \exists sk_{\text{vrf}} (u_{\text{label}}^{sk_{\text{vrf}} + 2^\ell \text{nonce} + 4ctr + \text{label} + 1} = g \wedge vk_{\text{vrf}} = g^{sk_{\text{vrf}}})$. Note in the above $\ell, \text{label} \in \mathbb{N}$, are public values, $ctr < 2^{\ell-2}$ always where ctr is the packet counter, nonce is a public random value that is produced after all other public values are committed. Recall that we use the numerical labels $\text{pkt} = 0, \text{type} = 1, \text{exit} = 2$.

In a nutshell, the above construction demonstrates that r is the output of the verifiable random function in a way that this can be verified with respect to counter ctr , public inputs label and n and the public key vk_{vrf} .

In order to engage in VRF routing, the client acquires a long term key $vk_{\text{long}}, sk_{\text{long}}$ associated with a compact e-cash wallet that can accommodate N unlinkable payments. We refer to this action as acquiring a “subscription” with N credentials. Subsequently the user registers with a gateway of her choice spending a credential and shares a key α that will be bound to the specific credential. The gateway, in turn, receives an allowance of packets to enter the mixnet equal to the sum of all credentials it receives in each period. To facilitate packet transmission, it registers a VRF key vk_{vrf} associated with each client’s credential it serves. Importantly note that, before registering each credential, the client is free to switch gateways without being tracked (due to the unlinkability of the compact e-cash scheme). At the same time, if the client is found to double spend a credential, this is traced back to her subscription vk_{long} that can be revoked, hence penalizing the misbehaving client.

Opening a measurement packet. A gateway and/or client can open a measurement packet corresponding

to a credential containing α by revealing the values $(ctr, r_{\text{pkt}}, \pi_{\text{pkt}}, r_{\text{type}}, \pi_{\text{exit}})$. In such case anyone can verify that this is a measurement packet corresponding to a counter ctr by checking that $r_{\text{type}} < T$ and the proofs. Moreover, the whole computation of such packet is possible to be verified as it can be derived from r_{pkt} . Observe that the packet is deterministically generated based on the values ctr, n, r_{pkt} . Regarding the size of the opening, observe we need one index, one group element, one hash and two exponents, for each of the three VRF openings. Using Ed25519, this amounts to 388 bytes per measurement packet opening.

Proof of no-skipping. For any counter value ctr that does not correspond to a measurement packet, a gateway can open the corresponding VRF value that determines this particular opportunity is a non-measurement legitimate packet. The gateway reveals the tuple $\langle ctr, r_{\text{type}}, \pi_{\text{type}} \rangle$ which can be verified against vk_{vrf} in conjunction to the test $r_{\text{type}} \geq T$. In a setting where all measurement packets have been opened, a random subset of the complement set of non-measurement counters can be challenged in this way to ensure that no measurement packets have been skipped. In more detail, if N is the number of proposed non-measurement packets, by opening v VRF values, the probability of missing all v times a skipped measurement packet is less than $(1 - 1/N)^v < \exp(-v/N)$. It follows that the probability of finding it is at least $1 - \exp(-v/N) = \alpha_{\text{ns}}$, i.e., we need $v = -N \ln(1 - \alpha_{\text{ns}})$. In terms of size of a single opening, observe that we need to reveal one index, one group element one hash and two exponents for the proof. Using Ed25519, this results to 132 Bytes per counter position.

Self-loops. A self-loop is a packet that a client sends to itself via the mixnet. In addition to acting as cover traffic that increases the privacy of the system (for more information on how self-loops play a role from this angle, see Loopix [29]), self-loops enable a client to verify the reliability of the gateway it has selected, in particular checking whether received packets are successfully delivered. For this, the client can trace the self-loop packets (but also any of its own packets) along the mixnet, and detect if the gateway is failing to deliver received packets (rather than those packets getting lost in transit). Note that the self-loops are essential only for testing the last leg of a packet’s routing to the receiving client. A client can move to a different gateway (with a new credential) if it finds the gateway’s reliability unsatisfactory.

Analysis. Given the above, the protocol augmented with VRF-based routing is extended by having gateways broadcast proofs of no-skipping, ensuring that all measurement packets are accounted for.

The first key observation is that conditioning on a legitimate packet being sent by the entry gateway, we obtain a coin flip with probability p_{lot} for sending a measurement packet. Due to gateways being utility maximizers observe that the total number of announced packets sent by gateway g , $N_g^{\text{gw}} = \sum_c N_{g,c}$ would be at least as large as the actual number of packets sent.

We next require that entry gateways open all the measurement packets in the announced ranges for each credential. Due to the proof of no skipping, any gateway that does not want to get caught lying must open all the measurement packets in the range for each credential it announced. More-

over, note that if there is a credential that is misreported to have been used less than in reality, e.g., the declared $N_{g,c}$ is smaller than the actual $N_{g,c}^a$, then there should be another credential c' that compensates for it by the same gateway, i.e., it holds $N_{g,c'}^a < N_{g,c'}$. It follows that for credential c' there will be measurement packets that have not being opened and hence this exposes the gateway g who will be caught in the proof of no skipping for credential c' .

Furthermore: (1) If measurement packets are not sent (despite being opened) this will reduce the performance of the gateway, so a utility maximizing gateway will not perform this action. (2) if non-measurement legitimate packets are selectively not sent (despite having the opportunity to send them) there are two possibilities: (i) the non-measurement packets are simply dropped, in which case client satisfaction drops and thus the gateway will not prefer this strategy; (ii) a gateway that colludes with the client may substitute legitimate packets by illegitimate packets that carry the same payload — this does not affect our estimation measurements that are only concerned with performance on legitimate packets.

For receiving gateways, assuming they are utility maximizers, we observe: (1) if measurement packet tags are not recorded by the gateway in the Bloom filter despite being received, the performance will drop, hence the gateway will not perform this action; (2) if non-measurement packets are not handed over to their destination this means that they have been processed, detected as non-measurement and then dropped. This affects client satisfaction (e.g, consider the case of clients sending self-loops) and as a result is not a preferred action of a utility maximizer gateway.

4 Node performance estimation

The goal of this protocol is to estimate, for every intermediary node j in the mixnet, a performance score $\hat{\rho}_j$ that reflects the rate of packet losses caused by j , with $\hat{\rho}_j = 0$ meaning that j lost all packets sent to it (e.g., if j is offline the entire epoch) and $\hat{\rho}_j = 1$ that the node was consistently online and correctly processed and sent all received packets. These $\hat{\rho}_j$ can be computed by any entity that knows the outputs of the sampling protocol described in Sect. 3, i.e., the amounts s_e^* and d_e^* of transmitted and dropped measurement packets per link $e \in G$. We consider reliable link transmissions such that any packet drops are either due to a failure of the predecessor or the successor. The estimated node performance $\hat{\rho}_j$ is computed as:

$$\hat{\rho}_j = \frac{\sum_{k \in S(j)} s_{(j,k)}^* + \hat{\beta}_{(j,k)} d_{(j,k)}^*}{\sum_{i \in P(j)} s_{(i,j)}^* + \hat{\beta}_{(i,j)} d_{(i,j)}^*} \quad (7)$$

In the case of gateways, $\hat{\rho}_g$ is computed considering the successfully transmitted (and dropped) measurements to first-layer successors $i \in S(g)$ (g ’s outgoing links); and the received (and dropped) measurements from last-layer predecessors $k \in P(g)$ recorded in their Bloom filter (g ’s incoming links).

The parameter $\hat{\beta}_e$ denotes the fraction of drops attributed to the link successor, with the remaining $1 - \hat{\beta}_e$ being attributed to the link predecessor. Ideally, participants verify

that $\hat{\beta}_e \approx \beta_e$, where β_e is the *actual* fraction of drops caused by the link successor. In a network deployment where packets are transmitted via point-to-point links $e = (i, j)$, it is however impossible for third parties to ascertain the true value of β_e , and thus $\hat{\beta}_e$ must be estimated based on knowledge on the patterns of node failure and the available evidence in the entire network. We thus consider the observable behavior of the two counterparties across all of their connections adopting a *threshold* approach to estimate $\hat{\beta}_e$.

Given the link performance estimates $\hat{\rho}_e$ for $e \in G$, computed according to Eq. 4, for a node j we define $\bar{\rho}_j^{\text{in}}$ as the median value of the incoming set of $\hat{\rho}_{(i,j)}$ for $i \in P(j)$, while $\bar{\rho}_j^{\text{out}}$ is the median value of the outgoing set of $\hat{\rho}_{(j,k)}$ for $k \in S(j)$. These median values for the incoming and outgoing edge sets are compared to a preset threshold $\bar{\tau}$. If node j 's median incoming (resp. outgoing) performance $\bar{\rho}_j^{\text{in}} \geq \bar{\tau}$ (resp. $\bar{\rho}_j^{\text{out}} \geq \bar{\tau}$), then j is considered to be functioning reliably on its input (resp. output) links; and unreliably otherwise. In this way, each node j receives a pair of labels, one for the set of input edges and one for the output set, each independently set to either *reliable* or *unreliable* depending on the node's median edge performance in each direction.

Given a link $e = (i, j)$, if both i 's output and j 's input are *reliable*, or both are *unreliable*, then any drops $d_{(i,j)}^*$ are symmetrically attributed to i and j (half to each with $\hat{\beta}_{(i,j)} = \frac{1}{2}$). If on the other hand one of the two is *reliable* while the other is *unreliable*, then the one identified as *unreliable* is attributed all the drops in that edge ($\hat{\beta}_{(i,j)} = 0$ if i 's output is *unreliable* and $\hat{\beta}_{(i,j)} = 1$ if j 's input is *unreliable*). This mechanism effectively identifies unreliable nodes subject to failures such as going offline or lacking enough throughput, as these failures affect the node's median performance. Additionally, in adversarial settings the malicious nodes engaging in selective packet dropping suffer as much performance degradation as they are able to inflict on their (otherwise reliable) targets.

We refer to Appendix C for further details on the rationale and implications of various approaches to assigning values to $\hat{\beta}_e$, and additional explanations why the threshold approach outlined above (and in more detail in Appendix C.3) offers the best tradeoffs.

Performance estimation in unreliable settings. We first consider scenarios where all nodes are non-adversarial but up to half of each layer may be unreliable, go offline, have limited throughput or otherwise be subject to random failures, and argue that the estimated $\hat{\rho}_j$ is a good approximation of the underlying ρ_j (given by Eq. 7 but using 'ground truth' s_e, d_e and β_e instead of s_e^*, d_e^* and $\hat{\beta}_e$).

Suppose that j is a reliable node that correctly receives, processes and forwards all packets. Then for any predecessor $i \in P(j)$, either $d_{(i,j)} = 0$, in case i is also reliable, or $\beta_{(i,j)} = 0$ if i is unreliable. With respect to successors $k \in S(j)$, either $d_{(j,k)} = 0$ in case k is reliable, or $\beta_{(j,k)} = 1$ if k is unreliable. It follows that $\rho_j = 1$. Assuming that at least half the nodes in every layer are reliable, since j is reliable and talks to a majority of reliable nodes in the preceding and succeeding layers, its median values $\bar{\rho}_j^{\text{in}}, \bar{\rho}_j^{\text{out}}$ are guaranteed to be above the reliability threshold $\bar{\tau}$, meaning that j is correctly labeled as *reliable*. If a

predecessor i or a successor k are unreliable, it holds that $\hat{\beta}_{(i,j)} = 0$ and $\hat{\beta}_{(j,k)} = 1$. This results in $\hat{\rho}_j \approx 1 = \rho_j$.

In case j is unreliable, observe that for reliable predecessors i and successors k , it also holds $\beta_{(i,j)} = 1 = \hat{\beta}_{(i,j)}$ and $\beta_{(j,k)} = 0 = \hat{\beta}_{(j,k)}$, which accurately attributes packet drops to j . On the other hand, if either i or k are unreliable as well, a disparity between downtimes with j can lead to a small deviation in the estimation $\hat{\rho}_j$ with respect to ρ_j (since the algorithm will set the $\hat{\beta}_{(i,j)}$ or $\hat{\beta}_{(j,k)}$ to $1/2$ thus averaging out both sub-par performances). We investigate this experimentally in Sect. 4.1.1 and demonstrate that we still obtain a good approximation $\hat{\rho}_j \approx \rho_j$ of the node performance score, with an accuracy that increases with the number of measurement packets.

Performance estimation in adversarial settings. We next discuss an adversarial setting where a colluding set of malicious nodes may drop packets to and from honest nodes that are the targets of the attack. The purpose of the attack is to cause the estimated performance of a target j (or set of targets) to be lower than its actual performance, i.e., $\hat{\rho}_j < \rho_j$.

Rather than obtaining an immediate benefit, an adversary engaging in such an attack may ultimately seek to harm the target's reputation to create opportunities for his own nodes [13]. For example, in Nym both the estimated performance and the amount of stake delegated to a node determine node participation and rewards. A lower estimated performance negatively affects node profitability, driving away the node's stake delegations – which adversaries may hope to attract for their own nodes. We aim to cause an adversary deploying this attack an aggregate degradation in estimated performance of adversarial nodes at least on par to the aggregate degradation suffered by the targets. If this is the case, the adversary fails to achieve its ultimate goal, since adversarial nodes will also exhibit poor performance and will also lose, rather than increase, their rewards, reputation and attractiveness to staking delegates, paying a price for engaging in the attack without any short-term or long-term benefits.

Consider j an honest reliable node being the target of the attack. Observe that as long as malicious nodes are less than half of a layer preceding or succeeding j , the best the adversary can do is drop packets directed to j in a way that both counterparties in the link will get the blame. This is due to the fact that the adversary cannot make j appear unreliable (since j is connected to a majority of other reliable nodes and hence its median values $\bar{\rho}_j^{\text{in}}, \bar{\rho}_j^{\text{out}}$ are above the threshold). It follows that the best strategy for the adversary is to ensure their nodes are reliable (by maintaining good performance in a majority of incoming and outgoing links) and lead the algorithm to the equitable $\hat{\beta} = 1/2$ choice of sharing blame between the two counterparties in each link it shares with j . In Sect. 4.1.2 we demonstrate experimentally this intuition and the proportionality of performance degradation between the adversary and the target nodes.

4.1 Simulation-based empirical evaluation

We have implemented a discrete-event mixnet simulator to empirically evaluate whether the proposed approach provides accurate performance measurement estimations in

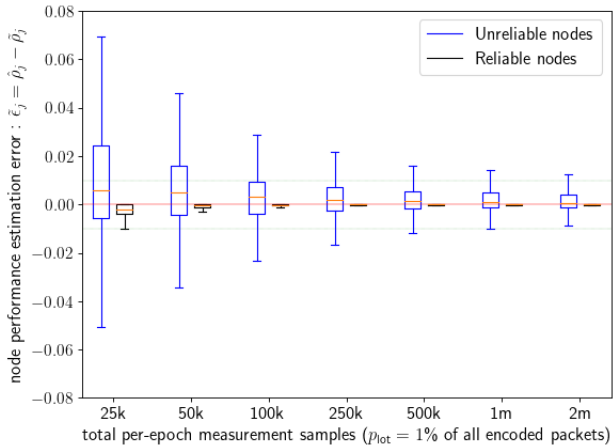


Figure 2: Distribution of error $\epsilon_j = \hat{\rho}_j - \rho_j$ for unreliable (blue) and reliable (black) nodes, for different amounts of measurement samples (from 25k to 2 million per epoch). We run 20 simulations per setup, each resulting in 320 values of ϵ_j (i.e., 6400 samples per pair of boxplots). Each boxplot shows the median (orange line), the first and third quartiles (upper and lower limits of the box), and the range of the distribution (whiskers); outliers are not depicted.

different scenarios. Simulation allows us to model various network conditions including reliable, unreliable and adversarial node behaviors, for which we know the ground truth, and compare the nodes’ true performance ρ_j to the performance $\hat{\rho}_j$ that is estimated based on the available measurement samples. We conduct an empirical evaluation of the estimation error $\epsilon_j = \hat{\rho}_j - \rho_j$ per node j , in both unreliable and adversarial settings. Appendix D describes in detail the implemented simulator, its outputs, the experimental setups used for the evaluation in unreliable and adversarial settings, and additional results for scenarios that combine both unreliable and adversarial participants.

4.1.1 Unreliable setting

We first evaluate the proposed node performance estimation protocol in scenarios where all nodes are honest but up to half the nodes in every layer are unreliable, as described in Appendix D.5. To evaluate the accuracy of the estimation given different amounts of measurement samples, we consider seven setups with between 25k and 2 million measurement packets in the epoch, corresponding to between 2.5 and 200 million total encoded packets for $p_{\text{tot}} = 1\%$. In each simulation run we compute $\epsilon_j = \hat{\rho}_j - \rho_j$ for every routing intermediary j . Figure 2 shows the resulting distributions of ϵ_j in each setup (aggregating samples from 20 runs), distinguishing between reliable (black) and unreliable (blue) nodes. Note that $\rho_j = 1$ for reliable nodes, and thus $\epsilon_j \leq 0$ for these, since their performance cannot be overestimated. For unreliable nodes, i.e., such that $\rho_j < 1$, the error ϵ_j can be positive or negative.

As we can see in the figure, the performance estimation error is small for reliable nodes (black boxes), and it becomes negligible once there are 100k or more measurement samples. In such scenarios, the proposed node performance estimation protocols are thus remarkably accu-

rate in their estimations for reliable nodes. The estimation error is larger for unreliable nodes, though it decreases as more measurement samples are available: with 25k samples the error range exceeds 7% of possible performance over-estimation and 5% of under-estimation, while this error range is within 1% of under- or over-estimation when 2 million measurements are used. Note that nodes are rearranged in the mixnet per epoch and measured independently in each epoch. Thus, we can expect that per-epoch performance estimation errors cancel each other out when averaging node performance over multiple epochs.

4.1.2 Adversarial setting

We now evaluate the proposed node performance estimation protocols in adversarial conditions. We consider that the adversary controls a set A of malicious nodes and wants to attack a set T of honest reliable target nodes, where $|A|$ and $|T|$ range from one node to up to 40% of two mixnet layers (32 out of 80 nodes in each layer). The details of the experimental setup can be found in Appendix D.6.

To attack a target node, an adversary node needs to share an edge with the target, either as predecessor or as successor. If the adversary is the successor of the target, then it simply drops packets coming from a target without registering them in its Bloom filter. If the adversary is the predecessor of a target, then it registers the received packet tags in the Bloom filter but then drops packets directed to the target, instead of actually sending them. The purpose of the attack is to degrade the measured performance of target nodes compared to their true performance. Thus, the adversary is more successful as the protocol more heavily underestimates the true performance of target nodes. The cost of the attack for the adversary is an ‘opportunity cost’ given by measured performance degradation suffered by adversarial nodes due to dropping packets for the attack. The attack is thus more costly as the protocol estimates a lower performance for adversarial nodes, compared to the performance that those nodes would have if they did not engage in an attack.

We run over five hundred simulations with various combinations of $|A|$ and $|T|$. In each experiment we compute the adversarial cost for the $|A|$ malicious nodes $c_A = |A| - \sum_{i \in A} \hat{\rho}_i$ and the cost imposed on the $|T|$ targets $c_T = |T| - \sum_{j \in T} \hat{\rho}_j$. Note that the overall attack scale increases proportionally to $|A| \times |T|$, as this determines the number of links where packets are dropped and consequently the magnitude of the attack costs c_A and c_T . This results in c_A and c_T values ranging from below 10^{-2} to above 10. We use log scale to represent results for the full range of values from small to large. In Figure 3 we show the result of each simulation as a dot with coordinates (c_A, c_T) . As we can see, all the results are close to the diagonal $c_A = c_T$, meaning that by engaging in this attack a set of malicious nodes take a combined performance penalty similar to the one they impose on the set of targets, even in scenarios where 40% of the targets’ predecessors and/or successors are adversarial. In the experiments shown in this section we consider that all honest nodes have perfect reliability and that all the packet drops are due to the attack. Appendix D.7 shows additional results where the network

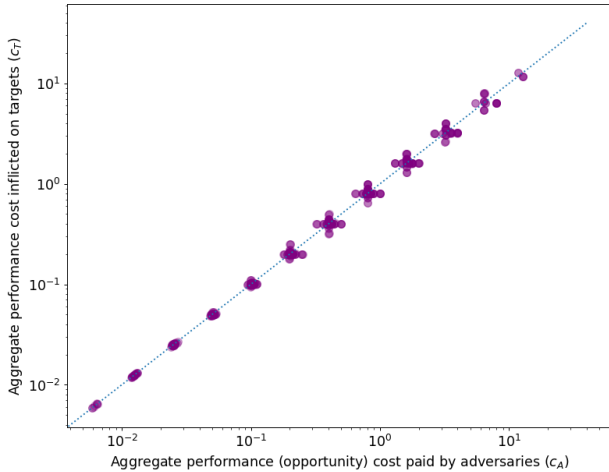


Figure 3: Results for adversarial settings where all honest nodes are reliable. Each sample represents the aggregate performance penalties c_T for $1 \leq |T| \leq 64$ targets (y axis) and c_A for $1 \leq |A| \leq 64$ adversaries (x axis) in each simulation run (total 510 runs).

includes both adversarial and honest but unreliable nodes.

4.2 Protocol overhead evaluation

In this section we evaluate the overhead introduced by the proposed protocols in terms of the amount of data that needs to be broadcast in each epoch, the data that needs to be stored long-term in a blockchain, and the computational overhead of VRF-based routing. We consider that a number of variables necessary for our protocols are already publicly available for the basic functioning of the mixnet, even before any performance measurement protocols are in place. This includes: parameters defining the mixnet topology, per-epoch selection and assignment of mix nodes to layers, node public keys (both for signing broadcast information and for decryption of packets), node staking and rewards, client subscriptions and information on spent client credentials. We thus focus on the additional overhead introduced by the proposed performance estimation protocol, summarized in Table 2.

We consider a setup with 100 million packets routed per epoch, of which 1 million (1%) are measurement packets. The mixnet includes 80 gateways and 240 mix nodes divided in 3 layers of 80 nodes. The data that needs to be broadcast in each epoch for computing performance scores includes:

Per-packet openings: Gateways broadcast an opening per measurement packet. Each opening has a size of 388 bytes. Considering one million measurements per epoch, this results in 388 MB.

Bloom filters: Each node must broadcast its Bloom filter at the end of the epoch. In the considered setup, a mix node is expected to route $1/80$ of the total traffic, amounting to 1.25 million packets. Considering a false positive rate of 10^{-5} , this would result in a Bloom filter with total size of 3.5 MB.⁵ Considering 240 mix nodes, their Bloom filters

⁵We use Bloom filter calculators available at <https://hur.st/bloomfilter/>

Ephemeral Storage	Per item	Amount	Total data
Packet openings	388 B	1 million	388 MB
Bloom filters mix nodes	3.5 MB	240	840 MB
Bloom filters gateways	300 KB	80	24 MB
No-skipping proofs	132 B	1 million	132 MB
Long-term Storage			
Node performance scores	2 B	320	640 B

Table 2: Overhead performance measurement protocol

would add up to 840 MB of data. The 80 gateways can have smaller filters, as they only need to record received measurements. Considering a false positive rate of 10^{-5} and a maximum of 100,000 received measurements per gateway, this results in 300 KB per gateway filter, adding up to 24 MB for all 80 gateways.

Proofs of no-skipping: Each opening for a position is 132 bytes; in our setup, we have 99 million packets in total per epoch. Consider a gateway who hides one measurement packet and does not open it. By requesting a proof of no skipping for $99 \cdot 10^6 \ln(1 - .01)^{-1} \approx 10^6$ non measurement positions, we have probability at least 1% for the gateway getting caught (for hiding even a single measurement). The Resulting size is 132 MB, and a cheating gateway will be caught after 100 epochs on average.

We consider that the computed performance scores for all nodes and gateways are stored long-term in the blockchain to act as a historical record of their measured performance. Considering a precision of four decimal places, this requires 2 bytes per node and gateway, resulting in 640 bytes for 240 nodes plus 80 gateways each epoch. Additional measurement protocol parameters that need to be available in the blockchain, such as p_{lot} and $\bar{\tau}$, may take a few extra bytes but do not need to be updated every epoch.

In terms of computational overhead, using the public benchmarks of Nym for Sphinx packet processing⁶ we obtain about 0.32ms per hop overhead in a standard linux server configuration. Extrapolating based on our implementation we observe that the VRF-based routing does add at most a Sphinx processing overhead to packet processing so the latency cost per hop in a similar configuration would still be under 1ms. Moreover, combining our scheme with Sphinx enables additional optimizations to further reduce this overhead. VRF-based routing also requires three VRF evaluations per packet that may be performed ahead of time as a preprocessing step, so that it does not impact packet transmission latency. If packets were created in real time rather than pre-processed, the three VRF operations would require about 1ms of additional computation. We note that with straightforward optimizations we can bring this cost down to a single VRF evaluation. Besides these negligible increases in latency due to VRF-based routing, note that our reliability estimation protocols do not increase the latency needed to route packets in real time, as all the time-consuming computations are done *a posteriori*, once the packets of an epoch have been delivered, rather than as part of packet routing. The protocols still should complete within an epoch, which should be easily feasible for epoch durations of one hour (as is the case in the current Nym

⁶See <https://github.com/nymtech/sphinx-bench>.

mixnet) or longer.

5 Related Work

First introduced by Chaum [4] in the early 1980s, mixnets are a key technique for anonymously routing packets that has inspired multiple lines of research that target different use cases for mixnets, each with its own tradeoffs.

Mixnets for voting applications. A key use case for mixnets in the literature is voting applications [27, 17, 35, 20], where the mixnet must ensure both the unlinkability of voters to their votes, as well as the integrity of the final tally. Therefore, in addition to privacy properties (input-output unlinkability), these solutions offer very high levels of assurance in terms of verifiability of correct behaviour by all participants, e.g.: each client is authorized by a credential to send a single well-formed ballot and verified to do so, while intermediary mix nodes are guaranteed to correctly process every packet without dropping, adding, or substituting any packets. This level of assurance is however achieved at a significant cost per routed packet: first, *all* transmissions between any parties happen “in public” via a broadcast channel (or “bulletin board”), so that everyone can verify who sent which (encrypted) packets at each step and no one can deny having received any packets (because they are all public); furthermore, every mix node must also produce and publish NIZK-based shuffle proofs of correctness for its published output packets [21], so that those outputs are considered valid and further processed by the next mix node along the route. The end-to-end latency and cost of this approach are acceptable in voting applications but is impractical for general-purpose internet access and other applications,

Mixnets for micro-blogging. Atom [22] is a mixnet designed to send short messages (as in micro-blogging) that provides similar reliability properties using lightweight traps. Atom can route one million 32-byte messages in 28 minutes, with latency growing with the number of routed messages and with message size. This is in contrast to the setup considered in this paper, where we expect the mixnet to route client messages with a size in (tens or hundreds of) KB within a second, independently of the number of client messages being routed. This is achieved in our design because the proposed performance estimation protocols are executed *a posteriori*, after all the messages of an epoch have been delivered, and thus have no impact on the processing time needed to deliver packets compared to the same mixnet *not* running our performance estimation protocols. Although Atom’s amount of broadcast data is not explicitly provided, given its design, the amount of required broadcast data grows with the number of client messages, in contrast to our approach, where the broadcast overhead remains constant for a given network size and measurement accuracy.

Mixnets for round-based private client messaging. A number of recent works has focused on solutions for private messaging via dead-drops for pairs of clients that exchange up to one message per *round*, which typically has a duration in the order of minutes. Vuvuzela [33] is able to route 240-byte messages with high throughput and a latency of

more than half a minute. It assumes that all servers are perfectly reliable: since it relies on a chain of servers, any one server being offline would render the messaging service unavailable to all users. Stadium [32] relies on verifiable shuffles for parallel mixnets that can scale to millions of users. While faster than Atom, the latency of messages is still in the order of minutes, and measuring mix server reliability is out of the scope of Stadium. XRD [23] proposes aggregate hybrid shuffles to improve efficiency over Atom while having the ability to identify mix servers that go offline or otherwise drop or substitute packets. Despite the performance improvements, XRD still has an end-to-end latency in the order of minutes that grows with the number of client messages being routed per round. Groove [1] introduces oblivious delegation mechanisms to allow clients to go offline without compromising their privacy properties – it however assumes that all mix servers are always online and does not discuss mechanisms to detect server failures or unreliability. Groove’s message latency is half a minute for one million users, and it also increases with the number of users. Karaoke [24] is the fastest design in this category, achieving a latency of 6.8 seconds for two million clients. The message transmission latency however still increases with the number of clients, reaching about half a minute with 16 million clients. Karaoke does consider network outages and malicious dropping of messages by adversarial mix nodes. It however only evaluates unreliability from the perspective of the impact of message drops on privacy properties (i.e., whether this may facilitate message deanonymization), and not from the perspective of service availability or mix node reliability assessments.

Mixnets for multiple applications. In this work we are most interested in mixnets that offer a flexible anonymous packet routing mechanism rather than being specifically tailored to a concrete application such as voting, micro-blogging, or round-based messaging. The earliest design proposing a low-latency general purpose mixnet dates from the early 1990s and is the ISDN-MIXes [28]. The design assumes a mix cascade topology and thus becomes unavailable if one of the mix servers goes offline. No mechanisms are proposed to counter or estimate packet drops. More recently, cMix [3] proposes mechanisms to reduce the message transmission latency by moving time-consuming public key operations to a pre-computation phase. cMix is thus able to route messages with sub-second latency. cMix’s reliance on pre-computation and cascades, however, makes it uniquely vulnerable to server failures, as clients sending a batch of messages would need to entirely redo pre-computation if just one of the nodes in the cascade fails either during the pre-computation or transmission phases of the round. cMix assumes servers are highly reliable and does not include mechanisms to evaluate their actual reliability.

Loopix [29] differs from previously mentioned designs in that it is not “round-based” i.e., processing and delivering packets in periodic batches – but “continuous-time” [19], i.e., processing packets individually, applying random delays at each mix that result in effective mixing [5]. Loopix was originally proposed as infrastructure for client messaging applications. The possibilities for clients tuning the average per-mix delay of their packets, and for the mix-

ing of packets with multiple latency distributions [18] (to suit different types of traffic), make Loopix flexible and configurable for low-latency applications, as is done in the Loopix-based implemented Nym network that we take as example system for deploying our solution.

Mixnet reliability. Finally, we review prior work that specifically tackles reliability in mixnets. Early research includes the proposal by Danezis and Sassaman [8] of having mix nodes send *heartbeat* traffic to themselves through the mixnet, similar to the *loops* of cover traffic implemented in Loopix, to detect active attacks by malicious nodes that drop or substitute messages. The idea of using reputation to increase the reliability of mixnets was already put forward in early work by Dingleline *et al.* [11], who proposed a solution that relies on semi-trusted third-party *witnesses* to verify whether mix nodes are correctly processing messages and help clients avoid under-performing nodes when choosing packet paths. This work however explicitly excludes active adversaries that try to compromise reliability measurements. Follow-up work by Dingleline and Syverson [13] eliminates the need for trusted witnesses by using test measurements and failure reports linked to reputation, as well as commitments to communal randomness, to build mix cascades that can detect dropped or substituted packets. This solution however suffers from “creeping death” attacks on measurements enabled by adversaries biasing the measurement protocol in their favor, such that over time honest nodes lose more reputation than adversarial nodes. Note that our solution avoids this problem by penalizing adversarial nodes symmetrically with respect to the reputational damage inflicted on their targets. Finally, more recent proposals by Leibowitz *et al.* [25] rely on honest mix nodes having perfect reliability (any packet loss is considered malicious), which is unrealistic in practical scenarios where honest participants may sometimes experience downtime or congestion. The goal of this solution is also slightly different from ours: to disconnect nodes that drop packets rather than to estimate their reliability in a decentralized manner.

6 Conclusion and Future Research

We have introduced a system where reliability estimates can be computed in an efficient and decentralized manner for a continuous mixnet’s links and nodes, given client credentials that authorize sending packets through the mixnet. To realize this concept, we put forward a *link performance estimation* protocol that uses covert measurement packets to estimate link performances for legitimate packets across the mixnet, and the associated primitive of *VRF-based routing* that ensures that legitimate client packets have routes chosen according to the mixnet’s routing policy, with malicious clients being unable to bias their packets. We further demonstrate how to use the link estimates as input to a *node performance estimation* protocol that allows mixnet participants to identify the under-performers amongst them.

Besides formally arguing the security properties of our new primitive, we have empirically evaluated via simulations the practical accuracy of the proposed protocols. To make our proposal practically relevant and easy to integrate with the currently deployed Nym mixnet, we consider 3 lay-

ers and 80 mix nodes per layer. We find that for this network size one million measurements are sufficient to provide accurate estimations for performance, with the number of required measurements remaining constant regardless of how many legitimate packets are routed. Our novel VRF-based routing primitive is however applicable to any other decryption mixnet with the two main required functionalities, namely issuance of credentials for authorized usage and a broadcast channel, e.g., a blockchain, available to all participants.

In comparison to most verifiable solutions, our solution is compatible with low-latency continuous time mix networks such as Nym as the verification steps happen *a posteriori* and thus do not add latency to the delivery of packets. Furthermore, the broadcast channel is used for a small fraction of packets (1% or less if the network routes several hundred million packets or more) rather than all of them. In addition, for each measurement packet only a few parameter values need to be broadcast to enable verifying the packet header, rather than requiring (as in e-voting oriented solutions) storing the entire packet including its payload, recorded repeatedly at each step of its route.

Our work can be extended in various ways. Future research includes protocols for free riding detection and additional mechanisms to protect against fully malicious gateways (rather than utility maximizer adversaries) that e.g., allow their clients to send (illegitimate) traffic without having a valid credential. Considering that the ratio of total to measurement packets received by each node provides information on whether a predecessor has only forwarded legitimate traffic, measurement packets can be used not only to estimate link and node performance, but also to detect traffic injection by mix nodes and gateways and uncover participants that engage in free riding or denial-of-service attacks. Blocklisting policies (and consequent loss of rewards and reputation) for mix nodes and gateways caught injecting traffic can be put in place to discourage malicious behaviour, though we note that these mechanisms may be social as well as cryptographic in nature. Finally, the use of digital signatures by gateways on client packets that act as receipt for clients can facilitate the public detection of malicious gateways that drop clients’ packets (even at the cost of their own utility, i.e., profit), by providing clients with evidence (in the form of a “promise to forward”) that can be verified by others. Note that clients can already use dummy loops [29] in our design to detect Byzantine dropping behavior by gateways, as the Bloom filter mechanism used in our scheme allows clients to trace their own packets (for which they know all packet tags) while maintaining unlinkability for all other clients.

Use of AI-based tools:

This work is entirely human-written without any assistance from AI-based tools.

References

- [1] Ludovic Barman, Moshe Kol, David Lazar, Yossi Gilad, and Nikolai Zeldovich. Groove: Flexible

- Metadata-Private messaging. In *16th USENIX Symposium on Operating Systems Design and Implementation (OSDI 22)*, pages 735–750, Carlsbad, CA, July 2022. USENIX Association.
- [2] Burton H. Bloom. Space/time trade-offs in hash coding with allowable errors. *Commun. ACM*, 13(7):422–426, jul 1970.
- [3] David Chaum, Debajyoti Das, Farid Javani, Aniket Kate, Anna Krasnova, Joeri De Ruiter, and Alan T Sherman. cmix: Mixing with minimal real-time asymmetric cryptographic operations. In *Applied Cryptography and Network Security: 15th International Conference, ACNS 2017, Kanazawa, Japan, July 10-12, 2017, Proceedings 15*, pages 557–578. Springer, 2017.
- [4] David L Chaum. Untraceable electronic mail, return addresses, and digital pseudonyms. *Communications of the ACM*, 24(2):84–90, 1981.
- [5] George Danezis. The traffic analysis of continuous-time mixes. In *Proceedings of the 4th International Conference on Privacy Enhancing Technologies, PET’04*, page 35–50, Berlin, Heidelberg, 2004. Springer-Verlag.
- [6] George Danezis, Roger Dingledine, and Nick Mathewson. Mixminion: Design of a type iii anonymous remailer protocol. In *2003 Symposium on Security and Privacy, 2003.*, pages 2–15. IEEE, 2003.
- [7] George Danezis and Ian Goldberg. Sphinx: A compact and provably secure mix format. In *30th IEEE Symposium on Security and Privacy (S&P 2009), 17-20 May 2009, Oakland, California, USA*, pages 269–282. IEEE Computer Society, 2009.
- [8] George Danezis and Len Sassaman. Heartbeat traffic to counter (n-1) attacks: red-green-black mixes. In *Proceedings of the 2003 ACM Workshop on Privacy in the Electronic Society, WPES ’03*, page 89–93, New York, NY, USA, 2003. Association for Computing Machinery.
- [9] Claudia Diaz, Harry Halpin, and Aggelos Kiayias. The Nym Network. Whitepaper of Nym Technologies SA, version 1.0, February 2021.
- [10] Claudia Diaz, Harry Halpin, and Aggelos Kiayias. Reward Sharing for Mixnets. *Cryptoeconomic Systems*, 2(1), jun 13 2022. <https://cryptoeconomicsystems.pubpub.org/pub/diaz-reward-sharing-mixnets>.
- [11] Roger Dingledine, Michael J Freedman, David Hopwood, and David Molnar. A reputation system to increase mix-net reliability. In *Information Hiding: 4th International Workshop, IH 2001 Pittsburgh, PA, USA, April 25–27, 2001 Proceedings 4*, pages 126–141. Springer, 2001.
- [12] Roger Dingledine, Nick Mathewson, and Paul Syverson. Tor: The second-generation onion router. In *USENIX Security Symposium*, pages 303–320, 2004.
- [13] Roger Dingledine and Paul Syverson. Reliable mix cascade networks through reputation. In *Financial Cryptography: 6th International Conference, FC 2002 Southampton, Bermuda, March 2002 Revised Papers 6*, pages 253–268. Springer, 2003.
- [14] Yevgeniy Dodis and Aleksandr Yampolskiy. A verifiable random function with short proofs and keys. In Serge Vaudenay, editor, *Public Key Cryptography - PKC 2005, 8th International Workshop on Theory and Practice in Public Key Cryptography, Les Diablerets, Switzerland, January 23-26, 2005, Proceedings*, volume 3386 of *Lecture Notes in Computer Science*, pages 416–431. Springer, 2005.
- [15] Jun Furukawa and Kazue Sako. An efficient publicly verifiable mix-net for long inputs. In Giovanni Di Crescenzo and Aviel D. Rubin, editors, *Financial Cryptography and Data Security, 10th International Conference, FC 2006, Anguilla, British West Indies, February 27-March 2, 2006, Revised Selected Papers*, volume 4107 of *Lecture Notes in Computer Science*, pages 111–125. Springer, 2006.
- [16] David M. Goldschlag, Michael G. Reed, and Paul F. Syverson. Hiding routing information. In Ross Anderson, editor, *Information Hiding*, pages 137–150, Berlin, Heidelberg, 1996. Springer Berlin Heidelberg.
- [17] Philippe Golle and Ari Juels. Parallel mixing. In Vijayalakshmi Atluri, Birgit Pfitzmann, and Patrick D. McDaniel, editors, *Proceedings of the 11th ACM Conference on Computer and Communications Security, CCS 2004, Washington, DC, USA, October 25-29, 2004*, pages 220–226. ACM, 2004.
- [18] Iness Guirat, Debajyoti Das, and Claudia Diaz. Blending different latency traffic with beta mixing. *Proceedings on Privacy Enhancing Technologies*, 2024:464–478, 04 2024.
- [19] Dogan Kesdogan, Jan Egner, and Roland Büschkes. Stop-and-go-mixes providing probabilistic anonymity in an open system. In *International Workshop on Information Hiding*, pages 83–98. Springer, 1998.
- [20] Shahram Khazaei, Tal Moran, and Douglas Wikström. A mix-net from any CCA2 secure cryptosystem. In Xiaoyun Wang and Kazue Sako, editors, *Advances in Cryptology - ASIACRYPT 2012 - 18th International Conference on the Theory and Application of Cryptology and Information Security, Beijing, China, December 2-6, 2012. Proceedings*, volume 7658 of *Lecture Notes in Computer Science*, pages 607–625. Springer, 2012.
- [21] Toomas Krips and Helger Lipmaa. More efficient shuffle argument from unique factorization. In *Topics in Cryptology—CT-RSA 2021: Cryptographers’ Track at the RSA Conference 2021, Virtual Event, May 17–20, 2021, Proceedings*, pages 252–275. Springer, 2021.

- [22] Albert Kwon, Henry Corrigan-Gibbs, Srinivas Devadas, and Bryan Ford. Atom: Horizontally scaling strong anonymity. In *Proceedings of the 26th Symposium on Operating Systems Principles*, pages 406–422. ACM, 2017.
- [23] Albert Kwon, David Lu, and Srinivas Devadas. Xrd: scalable messaging system with cryptographic privacy. In *Proceedings of the 17th Usenix Conference on Networked Systems Design and Implementation, NSDI’20*, page 759–776, USA, 2020. USENIX Association.
- [24] David Lazar, Yossi Gilad, and Nickolai Zeldovich. Karaoke: Distributed private messaging immune to passive traffic analysis. In *13th USENIX Symposium on Operating Systems Design and Implementation (OSDI 18)*, pages 711–725, Carlsbad, CA, October 2018. USENIX Association.
- [25] Hemi Leibowitz, Ania M. Piotrowska, George Danezis, and Amir Herzberg. No right to remain silent: Isolating malicious mixes. In *28th USENIX Security Symposium (USENIX Security 19)*, pages 1841–1858, Santa Clara, CA, August 2019. USENIX Association.
- [26] Silvio Micali, Michael O. Rabin, and Salil P. Vadhan. Verifiable random functions. In *40th Annual Symposium on Foundations of Computer Science, FOCS ’99, 17-18 October, 1999, New York, NY, USA*, pages 120–130. IEEE Computer Society, 1999.
- [27] C. Andrew Neff. A verifiable secret shuffle and its application to e-voting. In Michael K. Reiter and Pierangela Samarati, editors, *CCS 2001, Proceedings of the 8th ACM Conference on Computer and Communications Security, Philadelphia, Pennsylvania, USA, November 6-8, 2001*, pages 116–125. ACM, 2001.
- [28] Andreas Pfitzmann, Birgit Pfitzmann, and Michael Waidner. ISDN-mixes: Untraceable communication with very small bandwidth overhead. In *Proceedings of the GI/ITG Conference on Communication in Distributed Systems*, pages 451–463, February 1991.
- [29] Ania M Piotrowska, Jamie Hayes, Tariq Elahi, Sebastian Meiser, and George Danezis. The Loopix anonymity system. In *USENIX Security Symposium*, pages 1199–1216, 2017.
- [30] Alfredo Rial and Ania M Piotrowska. Compact and divisible e-cash with threshold issuance. *arXiv preprint arXiv:2303.08221*, 2023.
- [31] Alfredo Rial and Ania M. Piotrowska. Compact and divisible e-cash with threshold issuance. *Proc. Priv. Enhancing Technol.*, 2023(4):381–415, 2023.
- [32] Nirvan Tyagi, Yossi Gilad, Derek Leung, Matei Zaharia, and Nickolai Zeldovich. Stadium: A distributed metadata-private messaging system. In *Proceedings of the 26th Symposium on Operating Systems Principles*, pages 423–440, 2017.
- [33] Jelle Van Den Hooff, David Lazar, Matei Zaharia, and Nickolai Zeldovich. Vuvuzela: Scalable private messaging resistant to traffic analysis. In *Proceedings of the 25th Symposium on Operating Systems Principles*, pages 137–152, 2015.
- [34] David A. Wagner. A generalized birthday problem. In Moti Yung, editor, *Advances in Cryptology - CRYPTO 2002, 22nd Annual International Cryptology Conference, Santa Barbara, California, USA, August 18-22, 2002, Proceedings*, volume 2442 of *Lecture Notes in Computer Science*, pages 288–303. Springer, 2002.
- [35] Douglas Wikström and Jens Groth. An adaptively secure mix-net without erasures. In Michele Bugliesi, Bart Preneel, Vladimiro Sassone, and Ingo Wegener, editors, *Automata, Languages and Programming, 33rd International Colloquium, ICALP 2006, Venice, Italy, July 10-14, 2006, Proceedings, Part II*, volume 4052 of *Lecture Notes in Computer Science*, pages 276–287. Springer, 2006.

A Sphinx packets

Sphinx packets [7] are of the form $\alpha, \beta, \gamma, \delta$ where $\langle \alpha, \beta, \gamma \rangle$ is the header and δ is the packet’s payload.

- α is a group element g^x . It is used to derive a master packet key from the Diffie Hellman operation on α and the recipient’s public-key.
- β is a stream cipher ciphertext encrypted by extending a key derived by the master packet key. It hides the β', γ' part of the header for the next hop as well as the identity of the next recipient.
- γ is a MAC signing β with a key derived from the master packet key. At each processing step, the recipient verifier that the γ is a correct MAC on β .
- δ is a ciphertext encrypting the payload to be forwarded to the next hop. A symmetric cipher is used with a key derived from the master packet key.

When constructing a Sphinx packet one needs to determine the sequence of nodes n_1, \dots, n_ν for the path of the packet. Then the headers $\langle \alpha_i, \beta_i, \gamma_i \rangle$ are calculated. One key operation is that $\alpha_1 = g^x$, while for $i > 1$, $\alpha_i = (\alpha_{i-1})^{b_i-1}$ with b_i a blinding value calculated based on the master key of the i -th hop. It follows that the α values of the headers are calculated for $i = 1, \dots, \nu$. Once they are determined, the values $\beta_i, \gamma_i, \delta_i$ are calculated in the reverse order for $i = \nu, \dots, 1$.

B Proof of Theorem 1

Proof. (I) A key part in proving this statement is to demonstrate that the values used for the mixnet encoding \tilde{r}_i are indistinguishable to random values that the client would select independently of any public value. The mechanism is an extension of the Sphinx encoding and hence its security can be argued as in [7]. For completeness we provide the

main argument below. The main dependency is on the Decisional Diffie Hellman assumption and the random oracle model. For simplicity we argue first only the case that a single credential is used to send a single packet via a gateway. Consider the i -th hop of that packet. This involves the values $\alpha_i = \alpha_{i-1}^{b_{i-1}}$ and y_i , the public-key of the i -th node.

We show how to incorporate a challenge for the Decisional Diffie Hellman assumption $\langle g, a, b, c \rangle$ into the encoding calculation. We set the credential key α to be a and the node public-key y_i to be equal to b . It follows that the value \tilde{r}_i can be calculated as a function of the DDH challenge by $H(\text{rnd}, c^e)$ where $e = b_0 \dots b_{i-1} \cdot r_{\text{pkt}}$. Conditional on $e \neq 0$, it follows that \tilde{r}_i is uniformly random, unless the adversary queries the value c^e to the random oracle. Note that this event can only happen with non-negligible probability in the case the challenge $\langle g, a, b, c \rangle$ is a DDH tuple (as in the other case, the value c is random and hence can only be predicted with negligible probability by any polynomial-time algorithm). As a result, if the adversary queries c^e we can readily build a distinguisher by examining the random oracle queries of the adversary. Specifically, the distinguisher can test each query q for $q = c^e$ and output 1 if this is the case while producing 0 otherwise. It is easy to see that this algorithm will produce 1 with non-negligible probability when the tuple $\langle g, a, b, c \rangle$ follows the DDH distribution while it will produce 0 with overwhelming probability whenever $\langle g, a, b, c \rangle$ is a random tuple. Finally, observe that the probability that $e = 0$ is negligible given the randomness of the constituent values in the random oracle model.

The above argument generalizes via a hybrid argument in a straightforward manner to the case that there are multiple clients sending multiple packets. Note that it is in this step that the VRF property is needed since we want to ensure that the α_0 values of different packets appear independently sampled from the base group. The pseudorandomness property of the underlying function provides us exactly that: the value r_{pkt} would randomize α within the base group enabling us to repeat the DDH distinguishing argument for each packet.

Regarding privacy, our encoding mechanism introduces the values $\alpha_0, \alpha_1, \dots, \alpha_\nu$ that accompany each packet when they are sent over the network. As mentioned already, this is a sequence of blinded values that follow the Sphinx construction and hence the privacy proof would be identical. For completeness, the key argument is the following. Consider two values α_i, α'_i originating from the packet processing performed by a node in the $(i-1)$ -layer of the mixnet. We consider the two cases that these originate from the same credential containing value α or two distinct credentials containing values α, α' respectively. There are two exponents e, e' such that either $(\alpha_i, \alpha'_i) = (\alpha^e, \alpha^{e'})$ or $(\alpha_i, \alpha'_i) = (\alpha^e, (\alpha')^{e'})$. Indistinguishability boils down to the pseudorandomness of the e, e' exponents which relies on DDH and the random oracle model and can be argued in a similar way as above.

(II) The statement asks for the pseudorandomness of the values $r_0, \dots, r_{\nu-1}$, even in the case that the values vk, α, y_0 are adversarially chosen. Note that in this case we cannot rely on the DDH assumption or the properties of the VRF. Instead the key observation is that each value r_i

depends on the public nonce value via the random oracle as well as some other value s_i that as long as it is unique, r_i would be an independently sampled value. To prove this we consider the event that there are two values $s = g^e, s' = g^{e'}$ in this sequence that are equal, i.e., $e = e'$. Depending on the step when these values have been calculated the exponents will be a product of a number of values some of which are committed by the adversary, e.g., the discrete-log of the key of an adversarial gateway, the discrete-log of a credential's randomization key α as well as values produced by random oracle evaluations of such values e.g., the blinding exponents b_0, b_1, b_2, \dots and the keys of the mix-nodes. Conditional on no collisions in the random oracle $H(\cdot)$ or the VRF function, all these individual values involved in e, e' are distinct and, in case they are not outputs of the random oracle, are committed prior to the production of nonce. Based on this it follows that the event $e = e'$ would imply the event that $z_1 \cdot z_k \cdot h_1 \dots h_t = 1$ where h_1, \dots, h_t are random oracle outputs that depend on nonce and z_1, \dots, z_k values selected by the adversary. It is easy to see via generalized birthday problem [34] that this would require subexponential overhead in the worst-case (note in our setting t is a small constant).

(III) This statement follows easily due to the fact that the only difference between measurement and non-measurement packets is in the calculation of the α_0 value: in the case of a non-measurement packet this value is equal to $\alpha^{r_{\text{pkt}}}$, while in the case of a measurement packet it is equal to $g^{r_{\text{pkt}}}$. Given that client and gateway is assumed honest in this case, the exponentiation by the (hidden) value r_{pkt} results in a full randomization of the resulting element within the base group (with the precondition $\alpha \neq 1$); as a result the two cases are indistinguishable assuming the security of the VRF function. \square

C Approaches to setting $\hat{\beta}_e$

Here we propose and review three heuristic approaches to setting values for $\hat{\beta}_e$, which defines the fraction of drops d_e^* in link $e = (i, j)$ that are attributed to successor j , while the remaining $(1 - \hat{\beta}_e) \cdot d_e^*$ drops are attributed predecessor i . We assume reliable link transmissions such that no packets are dropped in link $e = (i, j)$ if both i and j are online and functioning correctly.

C.1 Naive approach: $\hat{\beta}_e = 1$

A simple approach is to “blame the receiver,” which corresponds to setting $\hat{\beta}_e = 1$ for all edges e . The rationale for this approach is that most of the hard work of processing a packet (deriving the decryption key and checking the packet tag for replay) is done by the time a node i is able to store the packet tag in its Bloom filter. Thus, if a packet is lost in link (i, j) , chances are that the blame is with j , who failed to be online or otherwise to process the packet. This naive model performs quite well in scenarios where all link drops are due to random failures by *honest but unreliable* nodes, since in practice chances are that the drop is due to the receiving end j being either offline or congested.

Such model is however easily subverted in a strategic adversarial setting: a malicious node i can selectively drop received packets (after storing their tag in the Bloom filter) destined to one or more target successors j , in order to unfairly degrade their measured performance $\hat{\rho}_j$. Given a mixnet with layer width W , an adversary that controls a set of $i \in A$ nodes in a layer can degrade the measured performance $\hat{\rho}_j$ of any number of nodes j in the succeeding layer, by up to $\frac{|A|}{W}$ at zero cost for the adversarial nodes in terms of lower measured performance $\hat{\rho}_i$ for malicious nodes $i \in A$.

C.2 Symmetric approach: $\hat{\beta}_e = \frac{1}{2}$

An alternative approach to penalize and discourage such adaptive malicious behaviour is to define node performance considering that half the ‘blame’ for drops in link $e = (i, j)$ is with i , and the other half with j , i.e., setting $\hat{\beta}_e = \frac{1}{2}$ for all links e . This symmetric attribution approach is effective at discouraging malicious packet drops as *any* drop now affects the performance of the adversarial node comparably to that of its target, which can be either a predecessor or a successor of the malicious node. We note that the symmetric attribution of drops however leads to an increasingly asymmetric performance penalty for large scale attacks involving many adversarial nodes and many targets. In such cases, $\hat{\beta}_e = 0.5 \forall e \in G$ begins to impose a larger performance penalty on link successors than it does on predecessors. This is due to successors receiving significantly less total traffic (due to the large scale nature of the attack) and thus the attributed half of the drops represent a larger fraction of the total inputs than for the predecessors, to whom the other half of drops are attributed.

A practical concern in cases where no attack takes place is that the symmetric attribution of blame results in a lowered performance $\hat{\rho}_i$ for the predecessors i of nodes j that are either offline or congested and unable to process all the received traffic – a scenario that may not be so rare. This may unfairly degrade $\hat{\rho}_i < \rho_i$ for reliable nodes i at the expense of overestimating $\hat{\rho}_j > \rho_j$ for unreliable nodes j .

Consider for example a case where $j \in F$ nodes in a layer of width W go offline shortly after processing a few packets, while all their predecessor nodes i are honest and reliable throughout the entire epoch, i.e., $\rho_i = 1$ for all nodes in the preceding layer. Attributing drops symmetrically causes $\hat{\rho}_i$ to be unfairly degraded by $\frac{|F|}{2W}$, while offline nodes j unfairly get credit for processing half the traffic sent their way, and their measured performance may be as high as $\hat{\rho}_j \approx \frac{1}{2}$ while in truth $\rho_j \approx 0$.⁷

C.3 Threshold approach: $\hat{\beta}_e \in \{0, \frac{1}{2}, 1\}$

The threshold approach aims to: (i) eliminate the unfair degradation of measured performance for reliable nodes due to successors being offline or congested, or predecessors being consistently faulty; while (ii) still symmetrically

⁷In the extreme case where a node j has zero measurement packets in its Bloom filter for the epoch, i.e., $\sum_i s_{(i,j)}^* = 0$, then the node is marked as having performance $\hat{\rho}_j = 0$. In this corner case all drops in the incoming edges (i, j) can be safely attributed to j and thus $\hat{\beta}_{(i,j)} = 1$ for j ’s incoming edges, while remaining $\hat{\beta}_e = \frac{1}{2}$ for the rest of edges e .

penalizing malicious nodes that conduct selective dropping attacks to degrade the estimated performance of honest, reliable predecessors or successors. This is achieved by assigning values to $\hat{\beta}_e$ that take into account node performance across its whole set of incoming or outgoing edges. The performance $\hat{\rho}_e$ of each edge is computed with Eq. 4.

C.3.1 Median incoming and outgoing performance

Given $\hat{\rho}_e = \frac{s_e^*}{s_e^* + a_e^*}$ for each edge e , we denote by $\bar{\rho}_j^{\text{in}} = \text{med}\{\hat{\rho}_{(i,j)} \text{ for } i \in P(j)\}$ the weighted median (i.e., 50% weighted percentile) of *incoming* link performance for node j , and by $\bar{\rho}_j^{\text{out}} = \text{med}\{\hat{\rho}_{(j,k)} \text{ for } k \in S(j)\}$ node j ’s median *outgoing* link performance. The node weight in the median computation is given by the share (relative to the full layer) of incoming or outgoing traffic routed by that node. In the case of links between mixnet layers, the node weight is determined by the routing policy. All the nodes in a layer count the same weight $\omega_j^{\text{out}} = \omega_j^{\text{in}} = \frac{1}{W}$ when the routing policy is uniform. This is not necessarily the case for gateways, whose weight is instead proportional to their share of sent measurement traffic received by mix nodes in the first layer (i.e., $\omega_g^{\text{out}} = \frac{\sum_i s_{(g,i)}^*}{\sum_x \sum_i s_{(x,i)}^*}$ when computing $\bar{\rho}_i^{\text{in}}$ for $i \in S(g)$), or received measurements from mix nodes in the last layer (i.e., $\omega_g^{\text{in}} = \frac{\sum_k s_{(k,g)}^*}{\sum_x \sum_k s_{(k,x)}^*}$ when computing $\bar{\rho}_k^{\text{out}}$ for $k \in P(g)$).

C.3.2 Threshold criteria

Let $\bar{\tau}$ be a threshold for the median performance that nodes are expected to achieve at a minimum when participating in the mixnet. The $\hat{\beta}_e$ is set per edge $e = (i, j)$ and it takes values in $\{0, \frac{1}{2}, 1\}$, according to the following criteria:

- $\hat{\beta}_{(i,j)} = 1$: if $\bar{\rho}_j^{\text{in}} < \bar{\tau}$ and $\bar{\rho}_j^{\text{out}} \geq \bar{\tau}$ (j has sub-par median incoming performance $\bar{\rho}_j^{\text{in}}$ while i has above-threshold outgoing median performance $\bar{\rho}_j^{\text{out}}$). If $\sum_i s_{(i,j)}^* = 0$ then $\hat{\beta}_{(i,j)} = 1$ for any value of $\bar{\rho}_i^{\text{out}}$.
- $\hat{\beta}_{(i,j)} = 0$: if $\bar{\rho}_j^{\text{in}} \geq \bar{\tau}$ and $\bar{\rho}_j^{\text{out}} < \bar{\tau}$ (j has above-threshold median incoming performance while i is showing low performance in more than half of its outgoing links).
- $\hat{\beta}_{(i,j)} = \frac{1}{2}$: if $\bar{\rho}_i^{\text{out}}, \bar{\rho}_j^{\text{in}} \geq \bar{\tau}$ (both i and j have above-threshold median performance), or $\bar{\rho}_i^{\text{out}}, \bar{\rho}_j^{\text{in}} < \bar{\tau}$ (both i and j have sub-par median performance).

Using median values $\bar{\rho}_j^{\text{in}}$ and $\bar{\rho}_j^{\text{out}}$ to infer whether a node is performing adequately across the board makes the approach robust to adversarial settings, up to the point where the adversary controls enough resources to affect median values. In the case of uniform routing and W nodes per mixnet layer this means controlling $\frac{W}{2}$ nodes in a layer; while in the case of gateways it involves controlling gateways that combined send half the total client traffic or that receive half of all the measurement packets.

Assuming that in every layer half the nodes are reliable, a reliable node j has median incoming performance $\bar{\rho}_j^{\text{in}} \geq \bar{\tau}$, as well as median outgoing performance $\bar{\rho}_j^{\text{out}} \geq \bar{\tau}$. In this

situation, any adversarial predecessor or successor that also has above-threshold median performance is penalized symmetrically with $\hat{\beta}_e = \frac{1}{2}$, taking upon itself as much blame for dropped packets as it inflicts on the target, which acts as a disincentive for the attack. If the adversarial node is instead underperforming in the median due to dropping too many packets, then the adversary receives *all* the blame for the drops, without affecting the performance of the reliable honest targets.

The $\bar{\tau}$ threshold also bounds the performance hit taken by reliable honest nodes due to non-malicious random failures of other nodes. One scenario is when a node j goes offline during the epoch, and thus fails to receive packets from all predecessors $i \in P(j)$ while offline. The threshold approach avoids penalizing all the well-performing predecessors i (that have $\hat{\rho}_i^{\text{out}} \geq \bar{\tau}$) for these dropped packets by setting $\hat{\beta}_{(i,j)} = 1$ for those links. Another likely scenario for non-malicious failure is *congestion*, i.e., a node j lacking the throughput to process all the packets routed through it, and thus failing to receive and process a non-negligible fraction of the packets sent by predecessors i . Due to widespread packet losses by j , we have again that $\hat{\rho}_j^{\text{in}} < \bar{\tau}$, and thus all the packet drops due to node j 's limited capacity are attributed to j rather than to its well-performing predecessors i , by setting $\hat{\beta}_{(i,j)} = 1$. Similarly, a node i with consistent faulty behaviour in its outgoing links (i, j) , i.e., with $\hat{\rho}_i^{\text{out}} < \bar{\tau}$ and a pattern of recording received packets in its Bloom filter but somehow consistently failing to successfully get those packets delivered to the next hop j , is also blamed for the drops $\hat{d}_{(i,j)}$, by setting $\hat{\beta}_{(i,j)} = 0$ on i 's outgoing links, so that reliable successors j do not take any performance hit from i 's consistently faulty behaviour.

C.3.3 Choice of threshold $\bar{\tau}$

The choice of value for $\bar{\tau}$ has the following effects. First, assuming that at least half of each layer is honest and reliable, the measured performance for a reliable node j is always $\hat{\rho}_j \geq \bar{\tau}$. Therefore, a higher $\bar{\tau}$ more tightly bounds the unfair blame that perfect nodes may receive in cases where multiple predecessors or successors perform *just* above the threshold $\bar{\tau}$. However, if the threshold performance $\bar{\tau}$ is too high to be attainable in practice, then many nodes will be in the 'underperforming' category. For nodes within this group, the performance hit due to others' drops is potentially much larger, since underperforming nodes are blamed by either half or all of the drops in their links (depending on whether the node at the other end of the link is also underperforming). In the extreme situation where all nodes fail to reach $\bar{\tau}$, the scheme behaves as in the symmetric approach. Thus, minimizing the impact on the measured performance for perfect nodes by setting a very high $\bar{\tau}$ comes at the expense of more likely and potentially larger performance impact for slightly-less-than-perfect nodes. In our experimental evaluations we use $\bar{\tau} = 0.99$ as threshold.

D Mixnet Simulator

This section provides a description of the simulator we implemented⁸ and used to conduct an empirical analysis of the proposed node performance estimation protocol. The scripts are in Python and use the SimPy library to handle events such as packet creation, packet sending, receiving and dropping. This section provides extensive details on the features, parameters and experimental setups we used in to obtain the results presented in previous sections, as well as additional experiments excluded from the main body due to page limits.

D.1 Clients and Encoded Packets

The simulator runs clients that encode and send packets throughout a simulated epoch of one hour. Packet generation by clients follows a Poisson process with a configurable rate of λ packets per second. Each encoded packet is a measurement packet with (globally configurable) probability p_{tot} . The rest are data packets addressed to other (randomly chosen) clients or cover traffic that clients send to themselves.

Packets routes are selected according to a uniform routing policy, considering a mixnet with $L = 3$ layers and $W = 80$ mix nodes per layer, as well as $W_G = 80$ gateways.⁹ We consider that legitimate client traffic is uniformly distributed over all gateways and also addressed in equal measure to recipients in all gateways. The encoded delay per packet per mix node is exponentially distributed with average 50ms, and we additionally consider 40ms of transmission time in each link and 2ms of packet processing time at the gateways.

D.2 Reliable, Unreliable and Malicious Nodes

In the simulations we treat gateways and mix nodes equally in terms of reliability, failure modes and malicious behaviour, and thus refer to all 80 gateways and 240 mix nodes indistinctly as 'nodes' that receive packets from their predecessors and forward them to their successors, sometimes dropping packets if they are adversarial or not fully reliable. Packets may be dropped by a node before or after the packet tag is stored in the node's Bloom filter. If a packet is dropped *before* storing, it is considered that the drop happened in the node's incoming link. If the drop happens *after* storing then it is accounted for in the node's outgoing link.

Nodes can have various types of behaviours:

- *Reliable* nodes are honest and function perfectly, meaning that they are always online and correctly process all the received packets without dropping any.
- *Unreliable* or *faulty* nodes are non-adversarial but subject to failures that cause packet drops. The possible

⁸The code can be made available upon request to reviewers and we plan to submit it for artifact evaluation.

⁹To make the simulations as realistic as possible, we select network and mixing delay parameters similar to those in the deployed Nym network.

failures include: (a) going offline for some (exponentially distributed) period of time, dropping any packets that were inside the node at the moment of going offline, as well as failing to receive new packets while offline; (b) becoming congested due to having a limited throughput and dropping packets on incoming links when the incoming packet rate exceeds the node’s throughput; (c) suffer from random glitches that cause packet drops in incoming or outgoing links with a certain probability.

- *Malicious* nodes are always online and have high throughput but they *purposefully* drop all or a fraction of packets in links with *selected* predecessor or successor targets, in order to degrade the performance estimates $\hat{\rho}_j$ for those targets.

D.3 Simulation Outputs

Once the epoch finalizes, the simulator logs in .csv files the outputs of the sampling protocol, including the s_e^* , d_e^* counts per link e as well as $\hat{\rho}_j$, $\bar{\rho}_j^{\text{in}}$, $\bar{\rho}_j^{\text{out}}$ estimates for every node j . In addition, the simulator logs packet counts for all edges and nodes that would not be available in an actual deployment – but that are available in a simulated environment and useful for evaluation purposes. This includes s_e , d_e , ρ_e , and β_e for all edges as well as ρ_j for all nodes and gateways. We evaluate the proposed performance estimation protocols by comparing the $\hat{\rho}_j$ output by the protocol to the underlying ground truth performance ρ_j , both in settings where packet drops are due to random failures and adversarial settings where packet drops are malicious.

D.4 Simulation Runtime

The runtime of a simulation is proportional to the number of packets encoded and routed in the full simulation. Each packet triggers a number of events, first as it is created by a client and then every time it is sent or received by an intermediary routing (or dropping) the packet. We perform simulations with a total of encoded packets between 2 million and 200 million, which require, respectively, between 15-20 minutes and 30-36 hours to complete. Simulations are CPU intensive (each simulation fully utilizes a CPU) but require little memory.

D.5 Experimental Setup: Honest but Unreliable Setting

In this setup we simulate scenarios where in each layer 40 nodes (half the layer) are reliable and the other 40 are (potentially) unreliable in various ways. To test the effect of different modes and degrees of failure we consider:

- 32 unreliable nodes per layer (40% of the layer) *may go offline* during the epoch. Each of these nodes toggles between being online and offline for exponentially distributed lengths of time, with average 90 minutes online and 10 minutes offline; i.e., on average, these nodes are online 90% of the time. Within a one-hour epoch however, about half of these nodes stay online

the entire epoch and in practice behave as reliable, with the other half going offline for at least part of the epoch.

- 4 unreliable nodes per layer (5% of the layer) have *limited throughput*, with one of them having a throughput equal to the average per-node incoming packet rate (and thus only dropping some packets when traffic is higher than average), and the other three having throughput that is $\frac{1}{2}$, $\frac{1}{4}$, and $\frac{1}{8}$ of the average incoming packet rate (and thus dropping, respectively, about $\frac{1}{2}$, $\frac{3}{4}$, and $\frac{7}{8}$ of the incoming packets).
- The final 4 unreliable nodes per layer (5% of the layer) *randomly drop* some packets. One of these nodes drops 1% of the incoming packets, another drops 1% of outgoing packets, a third drops 20% of incoming packets and the last drops 20% of outgoing packets.

We set the probability of a packet being a measurement to 1%, i.e., $p_{\text{lot}} = 0.01$. We vary the total amount of packets encoded by clients to study the node performance estimation accuracy relative to the number of measurement samples taken throughout the epoch. The results are shown in Figure 2.

D.6 Experimental Setup: Adversarial Setting

To simulate adversarial settings we consider scenarios with $A = \{1, 2, 4, 8, 16, 32, 64\}$ adversaries and $T = \{1, 2, 4, 8, 16, 32, 64\}$ targets. We only consider node assignments to layers that are most favorable to the adversary, i.e., where *all* A adversarial nodes are in layers *adjacent* to *all* the T targets, either as predecessors, as successors, or both. In cases where all A nodes are in a single layer, the T nodes may be all in the preceding layer, all in the succeeding layer or, for $T > 1$, distributed as $\frac{T}{2}$ in the preceding and $\frac{T}{2}$ in the succeeding layers. In cases where the A nodes are distributed among two layers, we consider that all T targets are in the layer between the adversaries, with $\frac{A}{2}$ as predecessors and the other $\frac{A}{2}$ as successors of the T targets. For 64 adversaries or targets we only consider scenarios where they are split over two layers (rather than all in one layer).

We consider that the A adversaries maximize the attack impact by dropping *all* (rather than just some) of the packets in the edges shared with the T targets – while not dropping *any* packets on edges shared with non-targets. Targets are reliable nodes that do not drop any packets and thus have a true performance of 100%. For the remaining ‘vanilla’ nodes, which are non-adversarial and non-targets, we consider two cases: one where they are all reliable (results reported in Section 4.1.2), and another where 30% of the nodes in each layer are potentially unreliable (results reported in Appendix D.7). The second case uses a setup almost identical to the one described in Section D.5, with the only difference being that only 16 (rather than 32) unreliable nodes per layer may go offline during the epoch.

In order to evaluate a large number of simulated scenarios within a reasonable time frame, we set $p_{\text{lot}} = 1$ in these simulations, meaning that in practice we exclude

non-measurement packets from the simulation. This speeds up by 100x the time needed to obtain experimental results without sacrificing accuracy of evaluation, since both targets and adversaries are considered to be reliable in the absence of attack and their measured performance loss is thus compared to having a reliable performance of 100%. Thus, simulating non-measurement packets does not add any useful information to the output while multiplying simulation time by 100. We consider scenarios with a total of 2 million measurement packets per epoch of one hour.

D.7 Experimental Results: Settings that Combine Adversarial and Unreliable Nodes

Here we examine scenarios where some nodes not involved in the attack are unreliable, as described in the experimental setup in Appendix D.6. Similar to the evaluation in Section 4.1.2, we compute the adversarial cost for $|A|$ malicious nodes as $c_A = |A| - \sum_{i \in A} \hat{\rho}_i$ and the cost imposed on the $|T|$ targets as $c_T = |T| - \sum_{j \in T} \hat{\rho}_j$. Each simulation run produces a result sample (c_A, c_T) that we represent as a dot in a scatter plot. We represent scenarios with large number of adversaries with a different symbol to better evaluate the impact of high corruption rates.

The results are shown in Figure 4, where we can see that adversary and target penalties are still symmetric in the majority of scenarios. We can see that $c_A \approx c_T$ in all scenarios below a certain scale. As the attack scale (proportional to $|A| \times |T|$) increases however, there are increased chances that unreliable nodes affect the measured performance of either adversaries or targets, making the attack cost asymmetric. This happens in particular when the combination of attack-related drops and unreliability affects the median incoming or outgoing link performance of a node, i.e., when more than half of a node’s incoming or outgoing links have sub-par performance for one or another reason. As explained in Appendix C, this makes the node be labeled as *unreliable* and increases the attribution of drops to that node. This can more easily happen to targets that are under attack from a large number of adversaries in an adjacent layer, as well as to adversaries that attack a large number of targets.

On the left side of Figure 4 above the diagonal we see a set of results for which the adversary succeeds in causing a large performance degradation on targets at no penalty to itself ($c_A \ll c_T$). This degree of adversarial success requires controlling 40% (32 out of 80 nodes) of at least one layer (all those samples are green ‘+’ symbols) but also some luck for the adversary. In various other instances with the same degree of adversarial control we observe that either: (i) the adversary has a penalty c_A that is lower than that of the targets’ c_T , but still proportional to it and non-negligible (row of green ‘+’ symbols over the diagonal for which $c_A < c_T$); (ii) the adversary’s penalty is symmetric with the target’s (‘+’ symbols on the diagonal for which $c_A \approx c_T$); or (iii) in a few cases the adversary pays a large penalty $c_A > 10$ without inflicting any penalty on the targets (‘+’ symbols on the bottom of the plot for which $c_A \gg c_T$).

The considered level of unreliability is not helpful for ad-

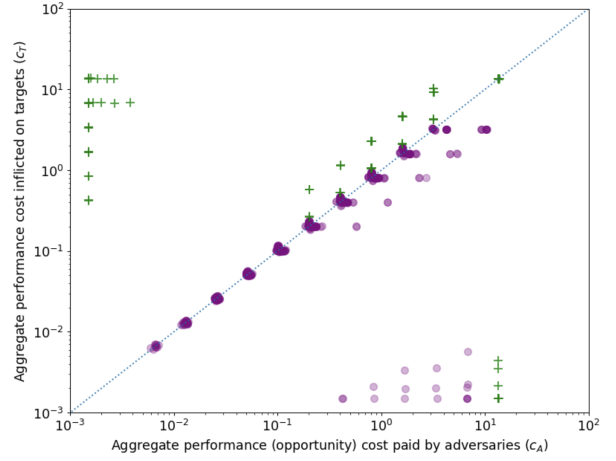


Figure 4: Results for settings with both adversarial and unreliable nodes. In the scatter plot each sample represents the aggregate performance penalties c_T for $1 \leq |T| \leq 64$ targets (y axis) and c_A for $1 \leq |A| \leq 64$ adversaries (x axis) in 630 simulation runs. Purple circles represent scenarios where adversaries control at most 20% (16 out of 80 nodes) of any layer. Green ‘+’ signs correspond to simulations where adversaries make up 40% (32 out of 80 nodes) of at least one layer.

versaries that control up to 20% of any layer (purple circle symbols). In these cases, at best the adversary pays a symmetric penalty (results on the diagonal, for which $c_A \approx c_T$), while in other instances it pays a higher cost than the target (circles below the diagonal for which $c_A > c_T$). In some instances the adversary pays a large penalty without the attack having an effect on the target (circles on the bottom of the figure for which $c_A \gg c_T$).